Neurosurg Rev (2003) 26:73–99
DOI 10.1007/s10143-003-0262-0

REVIEW

P. Grunert · K. Darabi · J. Espinosa · R. Filippi

Computer-aided navigation in neurosurgery

Received: 26 November 2002 / Accepted: 21 January 2003 / Published online: 10 May 2003

Abstract The article comprises three main parts: a historical review on navigation, the mathematical basics for calculation and the clinical applications of navigation devices. Main historical steps are described from the first idea till the realisation of the frame-based and frameless navigation devices including robots. In particular the idea of robots can be traced back to the Iliad of Homer, the first testimony of European literature over 2500 years ago. In the second part the mathematical calculation of the mapping between the navigation and the image space is demonstrated, including different registration modalities and error estimations. The error of the navigation has to be divided into the technical error of the device calculating its own position in space, the registration error due to inaccuracies in the calculation of the transformation matrix between the navigation and the image space, and the application error caused additionally by anatomical shift of the brain structures during operation. In the third part the main clinical fields of application in modern neurosurgery are demonstrated, such as localisation of small intracranial lesions, skull-base surgery, intracerebral biopsies, intracranial endoscopy, functional neurosurgery and spinal navigation. At the end of the article some possible objections to navigation-aided surgery are discussed.

Commentaries on this paper are available at http://dx.doi.org/10.1007/s10143-003-0263-z and http://dx.doi.org/10.1007/s10143-003-0264-y

And to thee, steerman, I give this command, and do thou lay it to your heart, since thou wieldest the steering oar of the hollow ship. From this smoke and surf keep the ship well away and hug the cliff, lest, ere thou know it, the ship swerve off to the other side and thou cast us into disaster.
Homer, Odyssey

P. Grunert (✉) · K. Darabi · J. Espinosa · R. Filippi
Department of Neurosurgery,
Johannes Gutenberg University,
55131 Mainz, Germany
e-mail: grunert@nc.klinik.uni-mainz.de
Fax: +49-6131-172274

Keywords History · Mathematical basics · Error estimation · Navigation · Digital localisation · Clinical application

Introduction

Since the very start of modern neurosurgery at the end of the nineteenth century, neurosurgical progress has been intimately related to improvements in intracranial localization. The knowledge of spatial relationships of lesions inside the cranium and the development of atraumatic approaches contributed essentially to reduced mortality and morbidity of neurosurgical interventions. Localization encompasses two questions: (1) where in the cranium the lesion or functional area must be assumed to be and (2) how to find this lesion or area during operation. This article will focus on the latter intraoperative aspect. The first question relates mainly to neuroradiologic developments and will be mentioned shortly first, because this imaging technique is also the basis and starting point for intraoperative localization methods.

At the beginning of our century, the topic of diagnostic localization of lesions could be understood only by analyzing the neurologic symptoms of the patient, without the possibility of referring to radiologic images. The first imaging technique, introduced by Dandy in 1918 [33], was visualization of the ventricles by direct injection of air and later of contrast medium into the ventricles or cisterna magna. From the shape and kind of ventricular displacement, lesions close to the midline structures could be detected. Later, in 1927, angiography was described by Egas Moniz [143]. This technique allowed localization of intracranial lesions either directly by visualization of the pathologic vessels or indirectly by associating the lesion with a lobe, depending on the characteristic frontal, temporal, or occipital displacement of the intracerebral arteries. Direct visualization of the cerebral tissue was not possible before CT was introduced by Hounsfield in 1973 [102].

Intraoperative localization technique, including positioning of the craniotomy and the direction of preparation, was based on knowledge of characteristic bony landmarks such as coronal suture, protuberantia occipitalis externa, etc., and the neurosurgeon's skill and 3D knowledge. As the operation proceeded, in particular at the skull base, identifying anatomic guiding structures, particularly cranial nerves, vessels, and characteristic bony landmarks, served as points of spatial orientation. This anatomic localization method was the gold standard not only before CT and MR imaging but also after their introduction. Microneurosurgeons used this detailed anatomic image information for better intraoperative identification of the anatomic structures and sophisticated planning of approaches [155, 156, 241, 242, 243, 244, 245, 246].

Parallel to the anatomic localization strategy, there was also the tendency from the beginning of neurosurgery to define the anatomic and pathologic structures in advance by using mechanical devices to define accurate approaches to targets and to provide objective information independent of the individual surgeon's skills. Frame-based stereotactic localization techniques were developed based on a rigid coordinate system in which the target and a straight trajectory were determined based on the image information. However, until recently microneurosurgeons were more comfortable with intraoperative anatomic identification than with stereotactic coordinates. The reason for this is not only that microsurgeons like to decide each step separately, depending on the changing anatomic situation in the course of operation but also because they trust more what they see rather than what computers calculate in abstract coordinates.

Frame-based and robotic technologies forced neurosurgeons to adapt their microsurgical techniques to the rigid stereotactic systems, which worked with high accuracy but reduced flexibility. Although frame-based stereotactic systems increased their intraoperative flexibility, it was computer-based navigation which, working interactively with images without visible coordinates and without instruments in the operating field, suited the visually and morphologically oriented neurosurgeons.

Definitions for interactive localizing techniques

At present, several terms are used for interactive localizing: computer-assisted surgery, computer-integrated surgery, computer-aided surgery, image-guided surgery, navigated surgery, and frameless stereotaxis.

Abdominal, head and neck, orthopedic, and ear, nose, and throat (ENT) surgeons prefer the term "computer-assisted surgery" (CAS), with "computer-integrated" or "computer-aided" surgery meant to cover a wide range of computer applications during surgery such as robotics, 3D rendering, surface simulations, and intraoperative localization. In this sense, the definition of CAS is too broad for neurosurgical purposes and does not characterize the neurosurgical applications. The aim is to define an operative technique which is basically microsurgical but makes use of advanced computer technology for better orientation during some parts of the surgical procedure. Therefore, frame-based stereotactic operations and robot-based interventions, which plan their complete approach in advance, will not be discussed in this article aside from their historical contributions. In neurosurgical literature, the terms image-guided surgery, navigated surgery, and frameless stereotaxy are more common for interactive computer-aided procedures.

The term image-guided surgery is too general, including by definition intraoperative imaging with ultrasound, CT, or MRI, which are not based on coordinate transformations and should be treated separately. On the other hand, frameless stereotaxy, in contrast to frame-based stereotaxy, indicates the frame as the main difference between classic stereotaxy and interactive computer-based localization. The essential difference between them is the different calculation of the position of the instruments in space and the interactivity with rapid real time visualization of the target point in the images and without use of a frame. There are even interactive localization devices that use frames to improve registration accuracy.

The imprecise metaphoric notation "navigated surgery" better describes the idea and aims behind this type of surgery. In Latin, "navigare" means to guide a ship on the sea. The interactive determination of the position during the journey was a presupposition for successful completion of a voyage. Apuzzo [6] pointed out the similarity of the basic concepts and the link, despite the shift in time, between nautical and cerebral navigation. In maritime localization, accurate cartography of islands and continents is just as necessary as atlases of the cerebral structures in neurosurgery. The interactive nautical localization was derived primarily from the positions of stars as fixed fiducials in the firmament. In Homer's Odyssey, we already find [98] a description of simple celestial navigation:

> And he sat and guided his raft skillfully with the steering oar, nor did sleep fall upon his eyelids, as he watched the Pleiads, and late-setting Bootes and the Bear, which man also call the Wain, which ever circles where it is and watches Orion, and alone has no part in the bath of Ocean. For this star Calypso, the beautiful goddess, had bidden him to keep on the left hand as he sailed over the sea. —Homer, Odyssey V, pp 270–277 [98]

By means of sextants, the positions of the stars were later measured with greater accuracy using a polar coordinate system with angles, azimuth, and declination. More recently, maritime orientation is based on satellite technology which detects and calculates with high accuracy any transmitter source on land or sea. Except for dimensions, the present GPS localization methods have very much in common with armless cerebral navigation using LEDs as emitter sources and a camera system for localization of a pointer tip in space. In nautical navigation, the visualization of the pointer tip in the corresponding CT/MR images corresponds to the direct visualization of one's own position on a map. The main difference between maritime and cerebral navigation is the change and displacement of anatomic structures during operation. The hypothetical marine analogy would be that, during a voyage, the cartography changes, making constant actualization of the charts necessary. This is exactly the problem in contemporary cerebral navigation and can be overcome only by intraoperative actualization of the image data [74, 236].

History of frame-based localization

Devices for the mechanical localization of intracranial structures go back to the beginning of modern neurosurgery. In Moscow, Zernow described in 1890 [55, 64, 251] an apparatus called an "encephalometer" which was fixed to the patient's skull and served to localize intracerebral structures based on superficial landmarks. His pupil Altuchow investigated the position of the basal ganglia using this encephalometer [5]. Actual stereotactic calculation based on a coordinate system was invented by Horsley and Clarke in 1906 [27] and 1908 [100]. They described a rigid frame attached to the skull which served as an immovable coordinate system in relation to which each point in the brain could be referred. They developed an arc system as a stable holder for introducing instruments to the target points, which were derived from brain atlases. This method was used only for experimental studies.

Stereotactic methods in humans were applied by Kirschner in 1933 [108] to puncture the foramen ovale at the skull base to treat patients with idiopathic trigeminal neuralgia. Stereotactic calculation of targets in the deep brain areas was, however, hindered in humans as opposed to animals by individual variations in the intracranial structures and by the lack of appropriate imaging techniques to visualize these variations.

Dandy [33] invented ventriculography in 1918 by performing an X-ray in a patient with an open, penetrating head injury and seeing the configuration of the ventricles filled with air. Then he described a method to introduce air artificially into the ventricles to investigate deep brain structures. Ventriculography was also the fundamental technique for calculating targets in the thalamus and basal ganglia because they have a stable and definite relationship to the topography of the third ventricle.

Spiegel and Wycis [207, 208] performed the first stereotactic thalamotomy in humans in 1947 using the commissura posterior or pineal body as an internal individual reference system. Functional operations with similar frames and techniques were introduced by Talairach 1949 in Paris [209], by Riechert in 1952 [170] in Freiburg, Germany, and by Leksell 1949 [122] in Stockholm for the treatment of extrapyramidal movement disorders, intractable pain, epilepsy, and psychiatric disorders.

After the development of CT technology by Hounsfield in 1973 [102] and Cormack [28, 29] based on mathematical solutions published by the Viennese mathematician Radon in 1917 [164], stereotactic coordinate-based calculation was applicable in the whole intracranial space, enlarging the field of indications to biopsies, interstitial brachytherapy, endoscopy, and localization of tumors for open surgery [7, 93].

Till the end of the 1980s, frame-based stereotaxy was the standard method for accurately localizing small intracranial lesions by introducing catheters into the tumors [15, 48, 49, 123] or for determining the tumor volume in space [107]. Coordinate transformation of the selected target point between the image and the frame space was established using a localization frame. Some of these stereotactic systems, for instance, BRW [228] and Cosman-Roberts-Wells (CRW) frames, used the rods of the localization frame for calculating a transformation matrix identical to the paired-point transformation method of frameless stereotaxy. The three oblique rods of the localization frame served as fiducial markers, which additionally made use of an optimal spatial arrangement.

History of frameless localization and robotics

The idea of frameless, interactive, computer-aided surgery consisted in navigation systems able to show in real time the position of the tip of an instrument in the corresponding images and not requiring a stereotactic frame for calculation. Because the navigation devices were basically adaptations of robot technology to surgical applications in regard to all the mathematical and technical knowledge necessary for real-time navigation, it seems justified to start the historical review with robots.

The concept of robots preceded its technical realization by 2,700 years and was described by Homer in the 18th chapter of the Iliad, when Thetis was visiting the god Hephaistos in Olympus to ask for new armor for her son Achilles [97]. Thetis observed two types of robots in the smithy: one type was machines on wheels which moved intelligently and automatically. The second type was androids of gold resembling girls equipped with the cognitive capacity of living creatures who helped Hephaistos in the smithy:

> Him she found sweating with toil as he moved to and fro about the bellows in eager haste; for he was fashioning tripods, twenty in all, to stand around the wall of his well-built hall, and golden wheels had he set beneath the base of each that of themselves they might enter the gathering of the gods at his wish and again return to his house, a wonder to behold. —Homer, Iliad XVIII, pp 372–378 [97]
>
> And he put upon him a tunic, and grasped a stout staff, and went forth halting; but there moved swiftly to support their lord hand-maidens wrought of gold in the semblance of living maids. In them is understanding in their hearts, and in them speech and strength and they know cunning handiwork by gift of the immortal gods. —Homer, Iliad XVIII, pp 416–420 [97]

Because such machines moved from internal impetus without external impulse, they were called automata[1]. The term automaton regained importance in the sixteenth and seventeenth centuries in Cartesian philosophy [38]. With the technical revolution in the eighteenth and nineteenth centuries, the ideas of automats were again very popular. People's fantasies were very similar to Homer's in wishing to build either machines or androids which would work instead of men. In the 1920s and 1930s, these androids were the starting point of a broad science fiction genre beginning with the Czech writer Karel Capek [23].

Capek also created the term robot. Robota means "to work" in Czech, and a robot (a machine working instead of a man by himself) was pictured by him in 1921 in a drama called "Rossum's Universal Robots." However, the first actual robots, called teleoperators, were developed in the Second World War to handle radioactive material and allow operators to perform tasks at a distance [70]. In 1949, the U.S. Air Force sponsored a program for a numerically controlled milling machine [185] which combined sophisticated servo-controlled systems with newly developing digital computer technology.

Before 1961, robots were not able to define their own position in space. At that time, tongs of a teleoperator slave arm were equipped with sensors to control the movements [185]. The first systems that could calculate their own position in space were developed in the late 1960s. Roberts [171, 172] demonstrated the possibility of defining the position of objects in space using a camera system and expressing their position and orientation by homogeneous coordinates.

The first robot driven by optical control was developed in 1967 by Wichmann [235]. Later, arm-based systems equipped with encoders to calculate angles in the joints were described by Pieper in 1968 [158]. He applied the theory of closed-link chains to obtain the mathematical solution for calculating the positions of device-related coordinates. These robots were able to calculate their own position in space and move to defined positions applying kinematic equations [37, 193].

Modified industrial robots with higher positioning accuracy were used in neurosurgery in the beginning of 1990s by Drake [43], Kwoh [117], Benabid [13], Fankhauser and Glauser [56, 67], Masamune [134], and Young [247]. In the middle of the 1980s, all the necessary mathematical and technical presuppositions existed for the realization of devices for navigated surgery:

1. Fast computers with appropriate data banks to handle image-based information in real time
2. Hardware and software for manipulators based on industrial robot technology with a high degree of accuracy
3. A high technical standard of image processing partly due to space research programs

[1] "Autos" means "self" in Greek

This technology had to be assembled in such a way as to satisfy surgical requirements. Passive manipulators, digitizers, and sensory arms which were able to determine their own position in space and transfer this information into images were introduced into neurosurgery in 1986 by Roberts [180]. He adapted a microscope for navigated surgery. It was equipped with ultrasound-emitting sources and microphones arranged outside the operating field. The microphone data were transported to a computer, which calculated the position of the microscope in space. The target point chosen on the CT/MR images could be projected into the ocular of the microscope and used for orientation during the operation.

In 1987 Schlöndorf [197] developed an arm-based system for ENT applications. This navigation system was later applied by Mösges [144] and Adams [1] to neurosurgical purposes. In 1987, Watanabe independently introduced an arm-based navigation system for neurosurgical operations [113, 230, 231]. In Switzerland in 1988, Reinhardt [165, 166] was working on an armless navigation system which used a pointer emitting ultrasound sources. Magnetic sources were also described later by Kato [105], and infrared light-emitting diodes (LEDs) as emitting sources by Zamorano [248]. Additional robotic capabilities were integrated into navigated microscopes by Giorgi [65] and Luber [126].

Basic principles of navigated surgery

To see the tip of a pointer in an image space, a relationship between the device space and the image space has to be established. This operation is called registration or calibration of the navigation device. Basically, a transformation matrix (T) has to be calculated which maps the coordinates of any point between the image and the device spaces. Techniques with different mathematics have been proposed:

1. Fiducial-based paired-point transformation
2. Surface contour matching
3. Hybrid transformation

Paired-point transformation

Paired-point matching uses corresponding sets of points whose coordinates must be established in the image and in the device-related space [182]. Most common are markers stuck to the skin [74, 176, 213]. Because these skin markers can shift, other more invasive solutions have been proposed to improve accuracy. Reinhardt [166] returned to a frame equipped with an array of sonic emitters fixed to a stereotactic frame, and Rousseau [186] put markers on the stereotactic frame to have fixed fiducials. Another possibility is to implant screws in the skull [19, 138]. Instead of artificial markers, corresponding anatomic structures can be also used as fiducials [51].

Such calibration is valid only if the patient does not move during surgery. To make possible intraoperative changes in patient position (as is common in neurosurgery during operation by moving the operating table with the patient fixed to the table in a rigid clamp), recalibration of the system is necessary. This can be solved by a dynamic referential frame consisting of an array equipped with LEDs which is fixed to the operating table. This solution provides only for relative changes of the operating table. Ryan [188] proposed to fix an LED array with a single screw directly to the skull of the patient to compensate for any displacement of the head during surgery. This problem is particularly urgent in ENT surgery, because the patient's head is not fixed at all during this type of intervention. Under these conditions, continuous recalibration using an array of LEDs fixed to the head is mandatory. Instead of an array, Kai [104] proposed the implantation of single LEDs as markers.

From a mathematical point of view, at least three paired points are necessary to establish a transformation matrix (T) between both spaces. If, however, homogeneous coordinates are used, which is common in robot technology, the number of fiducials has to be at least four. The basic equation (equation 1) for coordinate transformation can be expressed in compact form in matrix notation:

$$\underset{(X)}{\begin{pmatrix} x_1 & y_1 & z_1 \\ x_2 & y_2 & z_2 \\ x_3 & y_3 & z_3 \end{pmatrix}} \underset{(T)}{\begin{pmatrix} t_{11} & t_{12} & t_{13} \\ t_{21} & t_{22} & t_{23} \\ t_{31} & t_{32} & t_{33} \end{pmatrix}} = \underset{(X^*)}{\begin{pmatrix} x_1^* & y_1^* & z_1^* \\ x_2^* & y_2^* & z_2^* \\ x_3^* & y_3^* & z_3^* \end{pmatrix}} \tag{1}$$

The matrix (X) on the left consists of the *x*, *y*, and *z* coordinates of the three markers in relation to the device space. The transformation matrix (T) refers to the nine variables *t*, which have to be determined. On the right side of the equation is the matrix (X*) of the *x**, *y**, and *z** coordinates of the three markers in relation to the image space. The nine variables *t* of the transformation matrix can be calculated by multiplying matrices (X) and (T), leading to a system of linear equations which must be solved (equation 2):

$$\begin{aligned} x_1t_{11} + y_1t_{21} + z_1t_{31} &= x_1^* \\ x_2t_{11} + y_2t_{21} + z_2t_{31} &= x_2^* \\ x_3t_{11} + y_3t_{21} + z_3t_{31} &= x_3^* \\[1ex] x_1t_{12} + y_1t_{22} + z_1t_{32} &= y_1^* \\ x_2t_{12} + y_2t_{22} + z_2t_{32} &= y_2^* \\ x_3t_{12} + y_3t_{22} + z_3t_{32} &= y_3^* \\[1ex] x_1t_{13} + y_1t_{23} + z_1t_{33} &= z_1^* \\ x_2t_{13} + y_2t_{23} + z_2t_{33} &= z_2^* \\ x_3t_{13} + y_3t_{23} + z_3t_{33} &= z_3^* \end{aligned} \tag{2}$$

The matrix (T), applied to any point (*x*, *y*, *z*) in the device space, maps these coordinates of the pointer position in space into the corresponding coordinates (*x**, *y**, *z**) in the image space (equation 3). The inverse matrix, which can easily be determined from the matrix (T), maps in the opposite direction from the image space into the device space. The inverse matrix $(T)^{-1}$ is essential for microscope-based applications to visualize the target in the ocular of the microscope.

$$\begin{aligned} (x\ y\ z) \begin{pmatrix} t_{11} & t_{12} & t_{13} \\ t_{21} & t_{22} & t_{23} \\ t_{31} & t_{32} & t_{33} \end{pmatrix} &= (x^*\ y^*\ z^*) \\ xt_{11} + yt_{21} + zt_{31} &= x^* \\ xt_{12} + yt_{22} + zt_{32} &= y^* \\ xt_{13} + yt_{23} + zt_{33} &= z^* \end{aligned} \tag{3}$$

In case more than three fiducial markers are used for determination of the 3×3-dimensional transformation matrix (T), the calculation is overestimated and has in general no solution. Nevertheless, more fiducials are useful for selecting the best three fiducials (or four in case of homogeneity) which produce the smallest root mean square (RMS) error between both coordinate systems. The other possibility is to use all fiducials and reduce the amount again to three fiducials with new coordinates (*x***, *y***, *z***) under the additional boundary condition (equation 4) so that the square error of the whole overestimated linear equation system is a minimum. This so-called method of linear least squares was originally developed 1821 by the famous German mathematician K.F. Gauss for astronomical measurements of the orbit of the planetoid Ceres. This problem is, however, common in all empirical sciences with the number of observations higher than that of variables.

$$\begin{aligned} \|x^* - Xt\| &= \min \\ X^tXt &= X^tx^* \end{aligned} \tag{4}$$

Surface-based transformation

Surface-based transformations are iterative methods which, by continuous scaling, translation, and rotation, try to identify two rigid objects, applying optimizing criteria by minimizing the distance or a particular feature between both objects. They are understood as rigid body transformations (neglecting nonlinear inhomogeneities leading to image distortions in MRI) with six parameters, three of rotation and three of translation. The rotation is represented either by (3×3) Euler matrices (R1) (R2) (R3) using the Euler angles (equation 5) or by means of a (3×3) matrix (R*) of unit quaternions (equation 6) [119]. The translation in 3D space is represented by an additional vector V (*a*, *b*, *c*) with three variables.

$$R = \begin{pmatrix} \cos\alpha_3 & \sin\alpha_3 & 0 \\ -\sin\alpha_3 & \cos\alpha_3 & 0 \\ 0 & 0 & 1 \end{pmatrix} \begin{pmatrix} 1 & 0 & 0 \\ 0 & \cos\alpha_2 & \sin\alpha_2 \\ 0 & -\sin\alpha_2 & \cos\alpha_2 \end{pmatrix} \begin{pmatrix} \cos\alpha_1 & \sin\alpha_1 & 0 \\ -\sin\alpha_1 & \cos\alpha_1 & 0 \\ 0 & 0 & 1 \end{pmatrix} \quad (5)$$

$$q = (q_0\ q_1\ q_2\ q_3)^t$$
$$q_0 \geq 0 \quad q_0^2 + q_1^2 + q_2^2 + q_3^2 = 1$$

$$R = \begin{pmatrix} q_0^2 + q_1^2 - q_2^2 - q_3^2 & 2(q_1q_2 - q_0q_3) & 2(q_1q_3 + q_0q_2) \\ 2(q_1q_2 + q_0q_3) & q_0^2 + q_2^2 - q_1^2 - q_3^2 & 2(q_2q_3 - q_0q_1) \\ 2(q_1q_3 - q_0q_2) & 2(q_2q_3 + q_0q_1) & q_0^2 + q_3^2 - q_1^2 - q_2^2 \end{pmatrix} \quad (6)$$

Surface-based matching was originally described by Pelizzari in 1987 [152] and is well known as the “head and hat problem.” For applications in navigated surgery, the corresponding surface of the patient has to be matched with the appropriate 3D reconstruction from his images. The patient surface can be performed by selecting a sufficient number of points or lines with the pointer on the patient’s skin or with a laser contouring device [22, 72, 96, 211] which scans two-dimensionally and is able to recombine for a 3D contour of the skin. All mathematical realizations of this procedure try to minimize an abstract distance function D between both objects. This can be the Euclidean surface distance, voxel similarity, information entropy, mutual information, or other statistic functions such as for chamfer matching [120, 217, 250].

One problem of these iterative methods using functions such as distance or features which have to be minimized is the error due to local relative minima. This means that the algorithm stops the procedure if it reaches a relative but not necessarily the best possible matching.

Closely related to the matching technique for registration is the integration of different imaging modalities into the basic preoperative CT/MRI data set such as fluoroscopy in cases of spinal surgery [120] or functional data such as magnetoencephalography (MEG), transmagnetic stimulation (TMS), functional MRI (fMRI) [103], or actualization of preoperative imaging data with intraoperative CT, MRI, or ultrasound [236].

Hybrid transformation

Hybrid transformation combines surface-based and paired-point-based methods such as skin or bone surfaces with few implanted fiducials. Maurer [136] proposed the hybrid method to increase the surface-based matching accuracy by implantation of a single marker into the skull. The combination of both methods increases accuracy and reduces the amount of invasively implanted fiducials. Schmerber [194] published a hybrid registration method for ENT surgery matching anatomic skin and bone landmarks with skin and bone surfaces obtained from CT images. To diminish the invasiveness of the registration of bone surface points, instead of a needle he used a specific 1D ultrasound sensor as a transcutaneous telemeter. To calculate the six parameters (p) representing the appropriate rotation and translation, the boundary condition was expressed minimizing the least square energy function (E)p (equation 7).

$$E(p) = \frac{1}{M}\sum_{i=1}^{M}\frac{1}{\sigma_i^2}\left[\mathrm{dist}\left(S_{skin}T(p)P_s^i\right) - r\right]^2 + \frac{1}{N}\sum_{j=1}^{N}\frac{1}{\sigma_j^2}\left[\mathrm{dist}\left(S_{bone}T(p)P_p^i\right)\right]^2 = \min \quad (7)$$

Technical realizations of devices for navigation

The basic equipment common to all navigation devices is a pointer system and a computer work station. The computer consists of a digitizer for evaluation of the pointer position in space, a central processor for image processing, matrix calculation, and planning of the approach, and a high-resolution computer screen [11]. The pointer system, the referential frame, and, in armless systems, the detector unit are connected to the digitizer. The spatial information is transferred from the digitizer to the central processor, which additionally obtains CT/MR images via optical disc or direct net connection. For microscope-based systems [21, 58, 109, 173, 181], the information flow is also centripetal from the computer back to the ocular of the microscope to view the target point as an overlay, contours of the tumor, and orientation of the microscope axis to the target. Microscopes equipped with robotic properties also obtain instructions from the central processor about their motion in space [126]. (Fig. 1, Fig. 2). For microscope-based navigation systems, the focus distance corresponds to the mechanical pointer [54].

From a technical point of view, we can apply three independent classification schemata for the navigation systems:

1. Microscopes or mechanical pointers. In microscope-based systems, the whole microscope is the navigation device, and the focus distance of the microscope plays the part of the mechanical pointer.
2. Active robots or passive devices. Characteristic of the robots is their active computer-controlled movement.

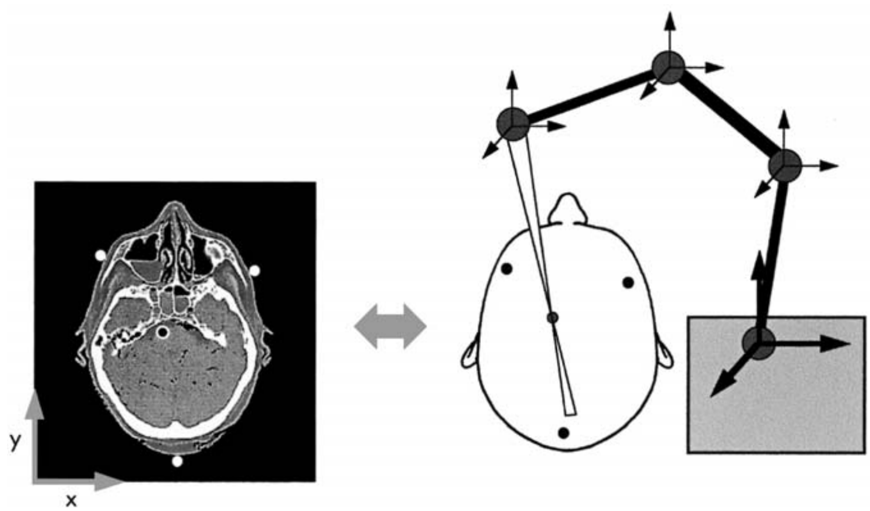

Fig. 1 Basic principle of an arm-based navigated microscope. The encoders in each joint measure the angulation. Together with the known geometry of the arms, these data are sufficient to determine its own position in space. The length of the focus serves as pointer tip. The spatial information of the focus tip is visible in the appropriate images, and the target point can be introduced as an overlay in the ocular of the microscope

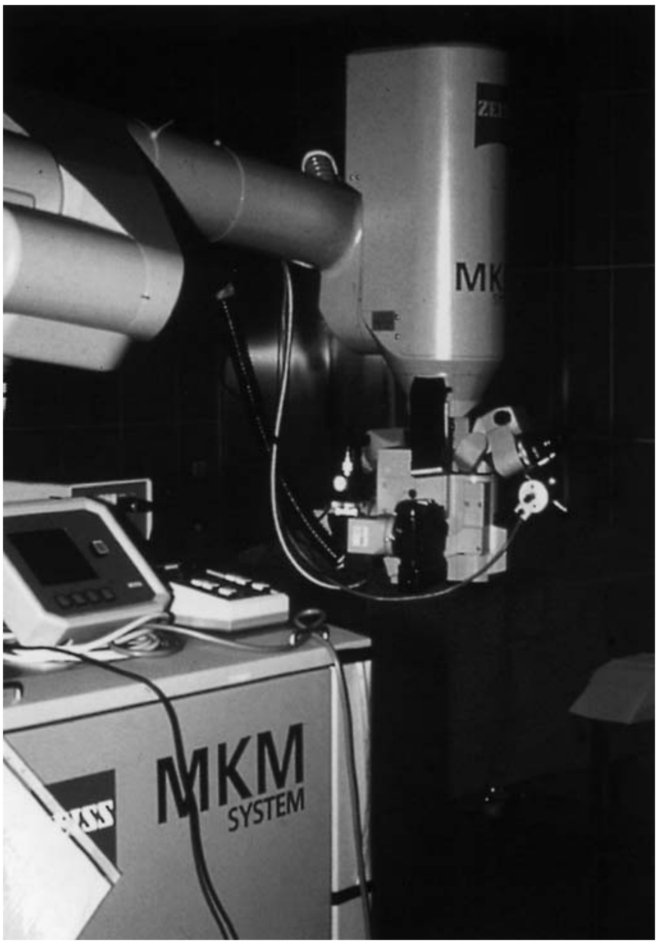

Fig. 2 MKM-navigated microscope with both navigational and robotic capabilities

The passive devices are however only able to determine their position in space and are otherwise moved by a person.

3. Arm-based or armless pointers. The distinction arm-based or armless refers to the method of determining the arm's own position in space. For the former, only one mechanical realization is possible.

For armless systems, further subdivision depending on the physical waves used as emitting sources into sonic, infrared, magnetic, and visible light waves is necessary. The sonic and infrared systems have active emitter sources fixed on the pointer, the magnetic-based systems use the pointer as the receiver, and the last method with visible light makes use of passive reflection of light on the objects of reference. Thus, together with the arm-based systems, there are five possible ways of technically determining the position in space. The precise classification of a navigation device includes the specification of the system regarding all three levels, which are independent of each other whether the device is a microscope or not, whether it an active robot or a passive device, and whether it is an arm-based or armless instrument.

For multiple coordinate manipulators (MKM), for instance, the correct technical specification would be: an arm-based, active microscope. The first level distinguishing between microscopes and other systems has two possibilities, the second level classifying robotic and passive arms also has two possibilities, and the last level as mentioned above has five realizations. This makes 2×2×5 or 20 technical combinations possible. All of them have been realized in modern industrial production.

Arm-based calculation of the device position

The arm-based systems consist of arms and joints with six degrees of freedom, three of translation (to arrive at each point in the space) and three of rotation (to reach the target from different angles) (Fig. 3, Fig. 4). The joints are equipped with sensory encoders to measure the angulation. This information is evaluated by the digitizer to calculate the position of the tip in space at a rate of

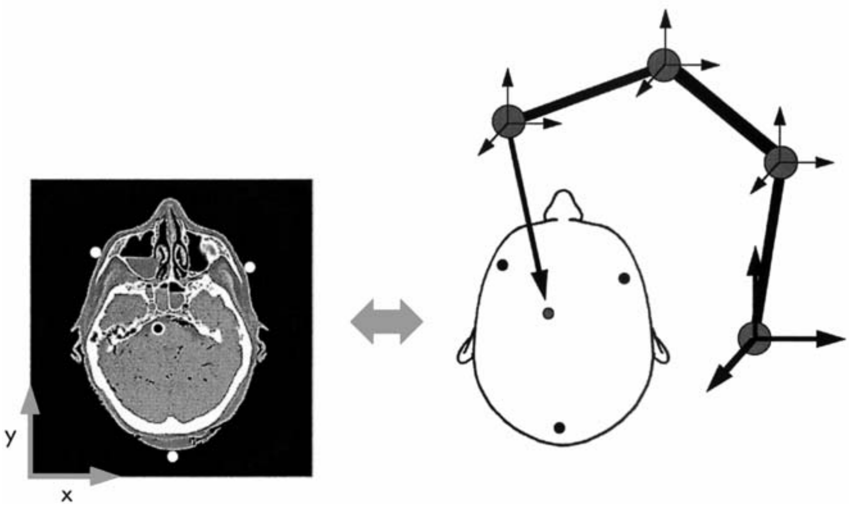

Fig. 3 Arm-based pointer device. The position of the pointer in space is calculated by the computer from the extent of angulation in each joint and from the length of the arms. Using skin markers for registration, the position of the pointer tip is visualized in the appropriate CT/MR image

Fig. 4 Intraoperative calibration of the operating arm system (OAS), an arm-based navigation device

30 positions/s to 300 positions/s. The position of the pointer tip in relation to the global coordinate system is expressed by the kinematic equation, which reflects the relationship between the position of the pointer tip to the relative position and orientation of the links. In matrix notation, displacement of the pointer tip from point A to point B in space is described as a successive multiplication of the six link-related matrices (A), each referring to displacement in the link-related position (equation 8).

$$(T6) = (A1)\ (A2)\ (A3)\ (A4)\ (A5)\ (A6) \tag{8}$$

In the case of robots with active movements, an optimal trajectory to the target point has to be calculated, taking into consideration not only the position but also the velocity and acceleration of the arm.

Armless calculation of the device position

The armless navigation systems determine their position in space by sonic, magnetic, or optic emitter sources which are fixed to a flexible pointer (Fig. 5, Fig. 6). The emitted waves are detected by microphones, magnetic sensors, or by means of an infrared camera array.

Ultrasound spark emitter sources send waves at constant frequencies of about 25 kHz. Travel time between the emitters and the receivers is measured using a synchronization technique. Provided the velocity of the

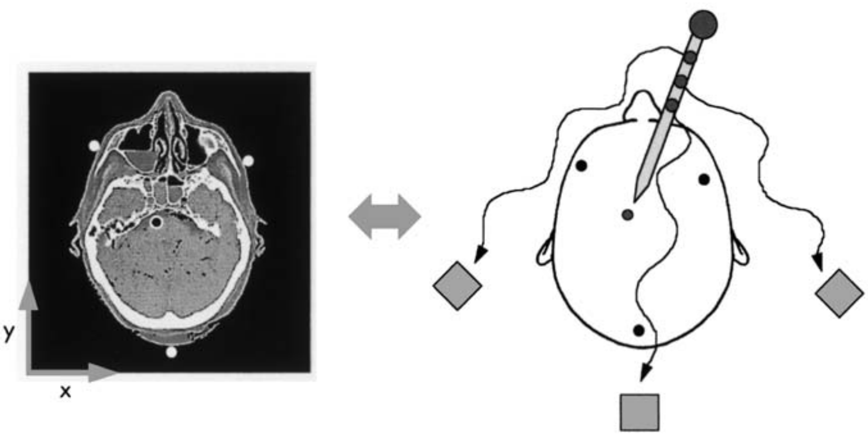

Fig. 5 Armless pointer device. The pointer is equipped with two or three sources emitting ultrasound, infrared, or magnetic waves. A camera or specific detector system outside the operating field detects the waves, and the computer calculates the position of the pointer tip. After registration, the tip of the pointer is visible in CT/MR images

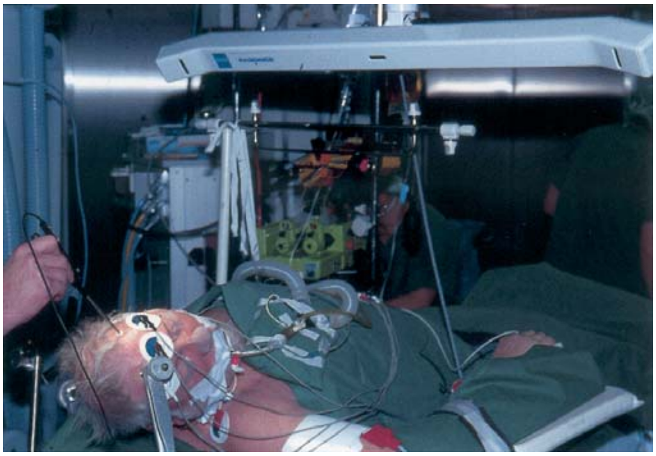

Fig. 6 Intraoperative calibration with the OTS. The patient is fixed in the Mayfield clamp. The pointer equipped with LEDs contacts the markers. The position of the LEDs is registered by the camera array

ultrasound in the air is constant, the distance between the emitter sources and the receivers can be computed knowing the geometry of the receivers and calculating the emitters as intersections of spheres centered at the receivers. The rate of measurements is in the range of up to 100 points/s.

Optic systems use a similar triangulation technique which allows one to determine a point in space from two cameras whose orientation and intercamera distance are known. The triangulation technique is named thus because the two cameras and the point in space to be determined form the vertices of a triangle. Charged-coupled two-camera devices (CCD) are able to calculate a point with a frequency of 300 points/s. To diminish irrelevant data in the input information, the camera system is pulse-synchronized with the emitter source's LEDs. Special position-sensitive camera devices (PSD) using cameras with analog PSD sensors are also in use. A third technique which minimizes data input involves at least three linear cameras. The spot on each 1D signal corresponds to a plane in three dimensions. The three cameras provide three planes in the space, and their intersection defines in space the coordinates of the desired point.

Some optically based devices use not emitting light sources for position measurement but only passive light reflected from the fiducials. The triangulation technique is again applied for determining the fiducial in space. The first passive visual light registration, so-called machine vision, was introduced by Heilbrun [94].

The magnetic navigation system consists of direct-current magnetic field generator, transmitter, and receivers detecting the magnetic field. Kelly [106] described a device using a transmitter with three orthogonal coils which generate a low frequency, 144-Hz magnetic field centered on the *x*, *y*, and *z* axes. A high-frequency field is not recommended because of nonlinear behavior of the parameters, with a subsequent decrease in spatial accuracy. As opposed to the optical systems, here the pointer is constructed as the receiver containing three coils measuring magnetic field strength. This information enables determination of the position of the stylus in relation to the emitting source and further to the global coordinate system.

A different solution was proposed by Hunnerup and Nielsen [103]. They used a transmitter fixed on a pointer and calculated its position by measuring the magnetic flux density at three fixed points and comparing them to a simulation model of the magnetic density flux. Because with one measurement of a sensor at a particular point, the localization of the emitting source had more than one solution, measurements with three sensors at different points were necessary. The intersection of curves created by the three sensors provided unequivocal results regarding the spatial position of the emitting source.

Accuracy of the navigation systems

First we have to specify and define the terms "precision," "bias," and "accuracy." Engineers use the term "precise" for a number of measurements whose standard deviation is small, although the mean (m) of these measurements is not necessarily close to the true value. The measurements are however unbiased if their mean value corresponds to the true value. Their standard deviation in this second case is not necessarily small, as is required for precision. A number of measurements are accurate only if they are precise and unbiased (Fig. 7).

In robot technology, two measurements of accuracy are common: repeatability and absolute position accuracy. Repeatability means the ability of the robot to perform the same motion and finish working at the same point. It reflects the precision of the system but not its accuracy, because the actual point does not necessarily coincide with the calculated point. Absolute position accuracy is a measure of coincidence of the pointer tip in space with the calculated coordinates. Robots usually have higher repeatability than absolute position accuracy. For navigated applications, only the absolute position accuracy is relevant.

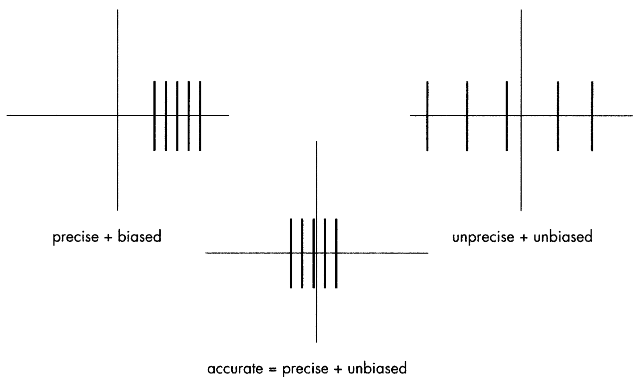

Fig. 7 Examples of precision, bias, and accuracy

A comparison of publications regarding the accuracy of the navigated devices is hindered by the different methods and parameters measured and the differing statistical evaluation, and even the unit in millimeters can differ, referring either to linear range error relative to the *x*/*y*/*z* coordinate axis or the euclidean distance *d* in space. It would be desirable to have a simple measure of accuracy for each device expressed as mean error in millimeters with a standard deviation which is independent of space and time during surgery. This simple reduction of the accuracy problem is however impossible for navigation systems.

We have to distinguish between three different types of accuracy, which are arranged here according to increasing complexity and sources of possible error:

1. Technical accuracy
2. Registration accuracy
   A. Phantom/cadaver measurements
   B. Intraoperative measurements
3. Application accuracy
A. Phantom/cadaver measurements

Technical accuracy indicates how reliably the navigation device can define its own position in space. The measurements are performed under standard laboratory conditions, and the error is valid in reference to a particular volume in space and the distance of the sensors from the emitting sources.

Registration accuracy relates to coordinate transformation. It depends on the technical accuracy of determining the fiducials by the navigation device and in the image space. We must separate measurements performed under laboratory conditions and those during the operation. The error is space- but not time-dependent.

Application accuracy reflects the overall error during the whole procedure. It includes technical accuracy, registration accuracy, and changes in the anatomic structures during the procedure. This error is time- and space-dependent. Again, we have to distinguish between phantom/cadaver studies and the intraoperative situation.

Technical accuracy

Technical accuracy is an interplay of two factors: the development of more accurate instruments and cost effectiveness, which is a compromise between the installation of more accurate instruments and the demand not to exceed particular financial limits. Important for establishing the required mechanical accuracy is the comparison of registration accuracy and application accuracy of the navigated devices and also the mechanical accuracy of the frame-based stereotactic systems.

The mechanical accuracy of the navigated devices should be higher than their registration accuracy and also be in the range of the frame-based stereotactic systems. It is meaningless to construct extraordinarily accurate mechanical, navigated devices which are extremely expensive and work with 100 times the mechanical accuracy of their subsequent registration and application.

The first arm-based navigation device of Watanabe in 1987 [230] had an error in absolute positioning accuracy of up to 5 mm. Roberts [180], describing the first microscope-based system in 1986, reported a mechanical error with a mean of 2 mm and range of 0.7–6.0 mm.

Along with arm-based systems, the main limitation in accuracy is the resolution of the encoders. Different technical solutions are available, such as potentiometers, optoelectric encoders, and resolvers. In general with digital optoelectric encoders, an accuracy of 0.022–1.3’ can be guaranteed over the full extension of 360° [145]. Defining a small working space with fewer angles, the accuracy can be further improved. Inside a 1-m working space, the technical accuracy of arm-based pointer systems is guaranteed by the manufacturers to be better than 0.6 mm. Maciunas [127] found a positioning accuracy within 0.1 mm in a space of 40×40×40 cm. In the clinical study of Zinreich [252], the technical accuracy was lower, with a mean of 1.12±0.61 mm.

From a technical point of view, the main advantage of arm-based systems is their robustness and independence from external influences such as temperature, air disturbances, surrounding objects, etc. They are however more difficult to use during operation and require more space in the immediate operating field than armless pointers.

Armless optic systems using the triangulation technique and charge-coupled two-camera devices (CCD), with 512×512-pixel image matrix resolution inside 1 m of working space and with a source camera distance under 2 m, are able to determine a point with an accuracy of 0.5 mm [145]. Increasing the distance between emitters and camera can significantly reduce the accuracy [145]. Position-sensitive devices (PSD) using two cameras with analog PSD sensors work in the same accuracy range. With three high-resolution cameras with a 4096×4096 image matrix calculating the intersection of three planes, the accuracy can be improved to 0.2 mm. The present passive optic systems working with high resolution cameras and without emitting diodes are also in the range of 0.3 mm.

With sonic instruments using a 24-kHz sound burst at a distance of 1 m, a mean accuracy of 0.89±0.63 mm (measuring the euclidean distance) can be achieved along with linear accuracy of better than 0.4 mm [101]. This accuracy can deteriorate under influences of temperature, moisture, and pressure. With appropriate measurement of these parameters, this error can be compensated [167]. Air disturbances under operating conditions additionally influence accuracy in the range of SD±1 mm [167].

Concerning the accuracy of navigation devices measuring the position in space from magnetic wavelet-emitting sources placed outside the cranial tissue, the tip of the pointer has an accuracy of 1.7 mm [105]. Because the magnetic flux density decreases in space by the power of three, leading to higher error in positioning accuracy due to high input data error, it is important to reduce the distance between the emitting source and the receiver.

With a strong magnet at a distance of 20–30 cm from the receiver, an accuracy of 0.76 mm is possible [103]. Additionally, the accuracy is sensitive to magnetic objects between the emitters and receivers and can deteriorate to 3–4 mm [105].

Using microscopes as navigation instruments, we have to consider the effect of the focus on accuracy, instead of the mechanical pointer. Westermann [232] showed that, with the optical overlay error into the ocular being 0.017–0.039 mm and the error due to zooming and focus setting being 0.04–0.11 mm, functional error was negligible in comparison to that from the simultaneously used optical tracking system, with a mean error of 0.3±0.15 mm and maximum of 0.76 mm [232]. For arm-based microscopes, the mechanical accuracy is a critical factor because of their large working space. To guarantee stability, these instruments require a special, massive construction. In general, for this type of robots the repeatability inside 1 m is 0.1 mm and the absolute positioning accuracy is 10 mm. By additional improvement and optimization of the parameters for each device individually, the positioning accuracy can be guaranteed to be within 0.5 mm.

With the present navigation systems, the contribution of technical error in the range of 0.1–0.6 mm is of subordinate value in comparison to the registration and application errors.

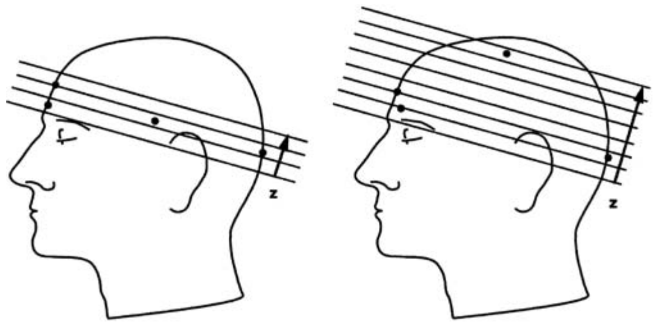

Fig. 8 On the left side, the arrangement is not correct in the *z* direction, leading to error amplification. On the right side, the fiducials are in correct placement, with no colinearity in the *z* direction

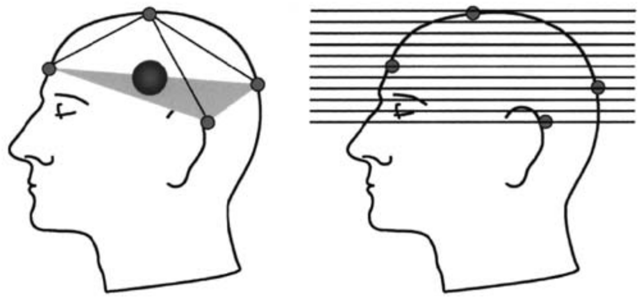

Fig. 9 As a rough estimate, the target area should be inside the polyeder, whose vertices are the fiducials

Registration accuracy

Registration accuracy measures the error due to matrix-based coordinate transformation between the device and image spaces. It answers the question of whether the cursor representing the tip of the pointer is correctly placed in the image space. Possible sources of limitation of accuracy in the device space using the paired-point matching method are:

1. Technical accuracy of the device
2. Type of markers (bone, skin, anatomic)
3. Form of the markers
4. Displacement of the skin markers
5. Determination of the center of the markers with the pointer
6. Determination of the center as focused by microscope

In the image space, the most important limitations are:

1. Resolution of the image given by pixel size in the *x* and *y* planes and slice thickness in the *z* direction
2. An accurate rectangular image data set
3. Movement of the patient in the gantry during data acquisition
4. Determination of the center of the fiducials
5. Type of imaging system—CT, MRI, digital subtraction angiography (DSA)

All errors cited above constitute the input data error for calculating the transformation matrix (T). The influence of this input data error between the device and image space on the calculation of the transformation matrix (T) and, in the next step, on the coordinates of the target point depends on two additional factors: geometric arrangement of the fiducials and position of the target in space (Fig. 8, Fig. 9).

The error amplification due to input data error depends strongly on the structure of the matrices X and X* (equation 1), which reflect the geometric arrangement of the fiducials on the head of the patient. In case the fiducials are colinear in the *x*, *y*, or *z* direction, the input data error can increase in the range of centimeters. Therefore it is important to avoid colinearity in any coordinate by placing one fiducial apart from all other markers (Fig. 8). The dependency of input data error on the position of the target point in space and on the arrangement of the fiducials was proven by Darabi [34] in a computer simulation. As a rule of thumb, the target area should be inside a polyeder whose vertices are the fiducials (Fig. 9). Under this arrangement, the error amplification is negligible.

All navigation systems based on paired-point transformation have a check for estimating the registration error. It is the root mean square (RMS) of the distance differences of the fiducials between the image and the device space (equation 9):

$$\sqrt{\frac{\sum (d^{*}N - dN)^2}{N}} \tag{9}$$

dN is the distance between two markers in the image space, and *d*N* is the distance between the same markers in the navigation space

The use of skin markers is most common in clinical application. The mean intraoperative RMS using CT with 2–3-mm slice thickness is in the range of 1.5–4 mm [74, 106, 146, 175, 176, 177, 213, 238]. With screws drilled into the bone, the accuracy can be improved because displacement of the markers on the skin during head fixation can be avoided. Brinker [19] measured an RMS of 0.23±0.03 mm with 1-mm CT slice thickness and screws drilled into the skull under experimental laboratory conditions. However, fixation into the skull is an invasive method. The possible displacements of the skin markers can be overcome by performing the CT intraoperatively after fixating the patient with the clamp [135]. As an alternative to skin markers, Maurer [137] proposed a hybrid method combining one screw with a surface-based transformation. With head fixation, the registration error was 0.7 mm and, without fixation, it was up to 1.4 mm.

Registration using anatomic landmarks seems to have the greatest registration error probably because of the difficulty to touch accurately the same corresponding points in the image and on the patient [95]. Villalobos [220] found the registration error intraoperatively (measured as the difference in the CT image between the marker and the cursor in the image space during pointing with the tip on the real marker) to be twice the error using self-adhesive markers: 3.4±0.4 mm compared to 1.6±0.1 mm. In Brinker's cadaver study [19], the relative difference between RMS using implanted screws and using anatomic landmarks was even higher: 0.23±0.03 mm vs 0.67±0.2 mm.

As an alternative to adhesive skin markers, subcutaneously implantable fiducials were proposed with the possibility of repeated use and which can be detected by ultrasound [124, 198]. Under experimental conditions, they work with an accuracy of 0.5±0.1 mm.

Surface-based registration depends on the technical accuracy of the contour scanning device, the method by which the 3D surface is created, the imaging technique with automatic feature-detecting algorithms, and the shape and geometry of the objects to be matched. The more anatomic structures with complex geometry such as facial structures are included, the better the matching. An error check is more difficult to obtain for surface-based registration than for the paired-point method. Measures which characterize only the degree of correspondence between both objects are insufficient. If additional anatomic landmarks or fiducials are used, RMS can be established. Bucholz [22] estimated the accuracy using a laser contour device with an optical tracking system in the range of 1.7 mm. Under experimental conditions, the RMS in his measurements was 0.5 mm. Maurer [137] found better results with paired-point registration than with surface-based registration (0.76 mm and 1.19 mm, respectively). Matching 200 randomly taken skin points and 17 bone points with 3D surfaces, Schmerber [194] obtained from CT images under experimental conditions a reported mean position error of 1.35 mm and an RMS of 0.71 mm.

Taking into consideration different markers and starting with the greatest error, the order of succession of the registration error seems to be: anatomic superficial landmarks, adhesive skin fiducials, surface matching, hybrid method with one screw, and screws in the skull. Exactly the opposite direction of this sequence relates to the invasiveness and necessary expenditure.

The imaging systems and the accuracy of determining the center of the fiducials in the image space contribute equally to the accuracy of registration [203]. It is obvious that an exact 3D data set of the images is a prerequisite for accurate registration. This means in particular that the patient may not move during image data acquisition. Therefore, in small children or uncooperative patients, imaging must be performed under general anesthesia.

Registration accuracy also depends on the imaging system, whether CT, MRI, or DAS [30]. It is well known that MR images can have spatial distortion due to nonhomogeneity of the magnetic field. These nonlinear effects have consequences on the accuracy of the determination of fiducials [36]. Maciunas [129] developed a correction algorithm which, applied to MRI, significantly improved the euclidean error in target registration between CT and MRI from 3.833±0.992 mm to 1.986±0.605 mm. Maurer [137] showed that the registration error could be significantly improved for paired-point registration and surface registration if the nonlinearity in the MR images is corrected. Thus, paired-point registration improved from 1.15 mm to 0.76 mm and the mean surface-based registration improved from 2.2 mm to 1.19 mm.

Evaluating application accuracy, Golfinos [71] found slightly better results with MRI than with CT. This surprising result could however be explained by the different slice thicknesses he used (3 mm for CT and 2 mm for MRI). Image resolution also plays an important part in registration accuracy. The resolution is determined in the *x* and *y* axes by pixel size, and the *z* coordinate is determined by slice thickness. Modern CT and MRI devices use a 512×512-pixel matrix, which corresponds to a resolution of about 0.5 mm.

Slice thickness comprises the crucial limitation in resolution. Under best conditions, the slice thickness is 1 mm. Using this optimal imaging resolution and screw markers, Brinker [19] was able to demonstrate the high accuracy in two cadaver procedures to the skull base, with mean RMS of 0.23±0.03 mm and 0.19±0.27 mm. Consistent with Brinker's study, Doward [41] found a significant improvement in accuracy using 2-mm rather than 3-mm slice thickness. He also confirmed the higher accuracy of CT over MRI. At the beginning of navigation, Watanabe [230] described in his original paper a navigated procedure using 10-mm slice thickness in consideration of stability of the images. With higher slice thickness, the images jumped on the screen to and fro. Most authors using skin fiducial markers use 2–3-mm slice thickness for cranial applications. At the skull base and when higher accuracy is necessary, 1-mm is preferable.

The determination of the center of the fiducials influences the accuracy of the registration. Usually the procedure is performed by free-hand technique. Because of the geometric form of the fiducials, it is more difficult to define the center than in frame-based stereotaxy using rods. However, correcting the position of the center in coronal and sagittal images helps to improve accuracy. Another possibility for improving accuracy consists in an algorithm which detects the fiducials automatically [229].

Finally, the learning effect also has to be considered. For microscope-based navigation, Rössler [176] observed an improvement in accuracy after the first 25 cases from a mean of 4.8±3.36 mm to 2.2±0.86 mm. The influence of the navigation devices on registration accuracy is not significant as long as the error due to the registration is much higher than the mechanical accuracy of the apparatus. With adhesive skin markers, Wirtz [238] obtained similar RMS results with an arm-based system, optical pointer, and multiple coordinate manipulator (MKM) microscope of 2.9±1.2 mm, 3.3±0.9 mm, and 3.1±1.0 mm, respectively. Registration accuracy is crucial in the whole navigation procedure. Under optimal conditions with appropriate markers and image resolution, the RMS can be as low as 0.2 mm. Using skin markers and 2–3-mm slice thickness, a mean RMS in the range of 1.5±3.0 mm can be expected under operating conditions.

The RMS is a reliable measure of registration accuracy only if the geometric arrangement of the fiducials is not colinear. Amplification of the input data error is not expressed by the RMS. To estimate the spatial relationship of the error, the best method consists in using additional markers or anatomical structures distributed equally over the head of the patient and checking their positions with the pointer after registration. If the fiducials are not arranged colinearly, the effect of error amplification can be ignored.

Application accuracy

Application accuracy is a measure of the targeting error during surgery. It answers the question of how reliably the pointer tip in physical space corresponds to its anatomic position in the CT/MR image during the procedure. In addition, the specific application error reflects the loss of correspondence between the image-based anatomic determination before surgery and the intraoperative anatomy encountered in actual physical space. The error is consequently not only space- but also time-dependent. Limitations in application accuracy are due to:

1. Technical inaccuracy
2. Registration inaccuracy
3. CSF leakage
4. Removal of tumor
5. Opening of cysts and ventricles
6. Tissue distraction by spatula
7. Displacement of the head in the clamp
8. Displacement of the dynamic reference frame (DRF)

Application accuracy is the most unpredictable factor of the whole navigated procedure because it depends highly on the specific intraoperative situation, in particular CSF leakage, duration of the operation, position of the head, and type, size, and location of the lesion. Therefore, when analyzing application accuracy, it is important to distinguish between cadaver studies and intraoperative measurements [239]. Using the umbo, asterion, and tympanic membrane as anatomic markers, Vrioni [221] found an application errors at the skull base between 0.91 mm and 2.44 mm. The results of studies on intraoperative application accuracy are also difficult to compare not only because they refer to different statistical parameters but especially because of their different measures for accuracy estimation.

Using skin markers for error estimation, Barnett [8] and Guthrie [81] found a mean error during surgery of 1.5±0.7 mm with a sonic pointer system. With the same method, Guthrie obtained a mean error of 3.3 mm and a range of 0.6–7.6 mm with an arm-based pointer system. However, skin markers reflect registration accuracy more than intraoperative application accuracy.

Golfinos [71] used bony landmarks intraoperatively as reference points to check the application accuracy. He used four measurements during the procedure. Immediately after calibration, the accuracy was better than 2 mm in 92% of MRI cases and 82% of CT cases. The error degraded during operation, and after the third evaluation it was less than 2 mm in 77% of the MRI cases and 62% of the CT cases. However, using bone landmarks checks the accuracy of whole head movements during surgery but does not relate to additional relative displacement of the brain structures in relation to the skull. Therefore, the application error of the intracerebral structures could be expected to be even higher. It would be more conclusive to use intracranial structures such as vessels, but the exact assignment between these structures and their correspondence in the image is difficult.

Thomas [213] measured the offset of the localized bone surface, cortex surface, superficial lesion margin, and tumor bed from the appropriate image positions, his mean results being 2.2±1.5 mm, 5.8±4.7 mm, 0.9±1.4 mm, and 2.9 ±4.5 mm, respectively. The high deviation at the cortex level is due to brain shift. However, more important is the finding that the error was very low at the level of the tumor margin. The same group evaluated application error in cases of stereotactic biopsy using postoperative MR images and image fusion. Dorward [41] found a mean linear error of 2.3±1.9 mm and a mean euclidean error of 4.8±2.0 mm.

For small lesions, the displacement of anatomic structures during operation is mainly due to CSF leakage. Immediately after opening the dura, application accuracy is in the range of registration accuracy and decreases with the course of time. How much CSF leaks depends on the position of the patient's head and the location of the craniotomy.

Dorward [40] measured a mean shift of the cortex surface of 4.6 mm after opening the dura, 5.1 mm after reaching the tumor margin, and 6.7 mm of the cortex at the end of the resection. In 28 investigated cases, Roberts [180] found an average displacement of 1 cm, with a dominant direction component associated with gravity. In a preliminary study, Mauerer [139] observed only little deformation of the midline and the hemisphere contralateral to the operation but shifting within 1 cm of the tumor and structures gravitationally above the surgical side. In our cases, displacement depended mainly on CSF leakage and the volume of the removed tumor.

Miga [142] developed a model update based on gravity-induced brain deformation. The error from brain shift could be improved from an average of 5.7 mm to 1.2 mm. The same group also published a mathematical method to update the CT/MR images by sparse data from digital cameras or ultrasound [66, 90, 174]. An alternative possibility is to perform intraoperative CT or MR images and replace or match them into the previous data set [114, 166]. Using intraoperative MR images, Wirtz [236, 237] actualized the image data and used them for navigation during the entire surgery including whole tumor resection. Another possibility is to use the open MRI or CT intraoperatively instead of navigation [4, 110, 214].

Summary regarding navigated accuracy

In conclusion, the error of technical device accuracy is low, in the range of 0.1–0.6 mm. The registration error is higher, depending on image resolution and the type of fiducials, being typically in the range of 0.2–3.0 mm. The application accuracy is the most unpredictable, depending on time, CSF leakage, and localization of the operation, being in the range of 0.6–10.0 mm.

Clinical applications

Tumor localization

Localization of small intracranial tumors is presently the most frequent application of navigated technology in neurosurgery for adults [8, 9, 35, 42, 44, 46, 52, 71, 74, 79, 81, 82, 83, 84, 88, 121, 127, 128, 140, 146, 148, 167, 168, 175, 176, 177, 178, 179, 190, 195, 199, 201, 205, 206, 212, 213, 218, 222, 223, 224, 225, 237, 238] and children [45, 85, 226]. It is used to decide the type of craniotomy and find the tumor atraumatically after dura opening. Typically on the day of the operation or 1 day in advance, CT/MR images with markers are performed without gantry tilt to obtain a Cartesian data set. The images are transferred to the navigation work station, and the patient is intubated and fixed with the head clamp. Then the registration is performed, taking around 10–15 min (Fig. 10). After calibration, the pointer is moved slowly over the patient's scalp and the corresponding cursor of the tip is observed moving in real time in the appropriate axial, coronal, and sagittal images. The best position of the craniotomy is decided and, if necessary, additional superficial anatomic structures such as sagittal and transverse sinus can be defined and drawn on the scalp. With an extension function or by sliding the LED holder more closely to the pointer tip, the trajectory to the lesion can be visualized. After craniotomy, the pointer is used to decide the corticotomy and the direction to reach the lesion. For very small or deep-seated tumors with long access to the tumor through the gray and white matter, a catheter can also be implanted through the pointer, which itself is fixed in space by two Laila arms or a special instrument holder [41]. The most frequent clinical indications for navigated localizations are small meningeomas [10], gliomas [130], metastases [83] (Fig. 11), and cavernous hemangiomas [216] (Fig. 12).

Fig. 10 Intraoperative registration with the OAS. Five skin markers are visible in the frontotemporal area

The delineation of tumor borders is in general no more accurate if brain shift must be assumed. Nevertheless, the navigation rules out overlooking big tumor remnants. To improve intraoperative accuracy, additional intraoperative image actualization is necessary. The navigation can also be helpful in delineating superficial low-grade astrocytomas at the beginning of the operation while investigating the cortical surface (Fig. 13) and also in subtemporal transtentorial approaches for resecting the tentorium at the proper place. Using a navigated microscope, the spatial information of the tumor and its borders are directly overlaid into the ocular.

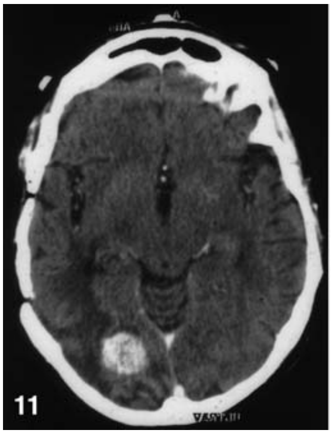

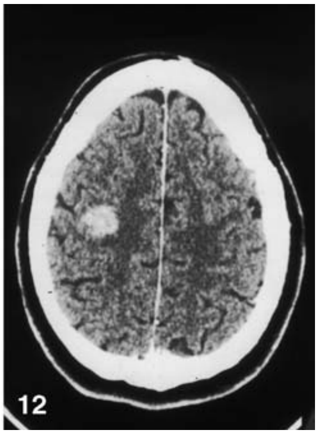

Fig. 11 Computed tomographic image with a metastasis in the right occipital region which was localized by navigation
Fig. 12 Computed tomography of a hemangious cavernoma in the right frontal lobe close to the motor strip

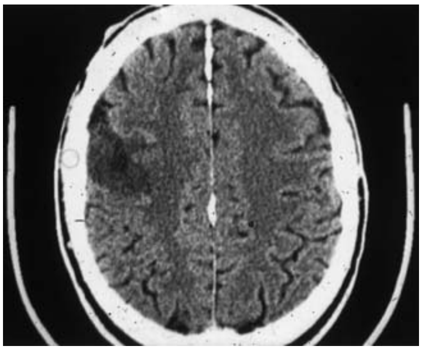

Fig. 13 Computed tomography of a low-grade astrocytoma in the right frontal region. *Circle* shows the actual position of the pointer tip

Skull-base surgery

From a technical point of view, skull-base surgery is an ideal application of navigation because no intraoperative shifting is to be expected. Ear, nose, and throat surgeons therefore use navigation as an orientation aid for nasal, paranasal, and otologic interventions [26, 89, 91, 92, 204, 232, 233, 234]. In cases of tumor surgery, navigation is usually not necessary for finding lesions, because there are enough anatomic landmarks for orientation, but it helps estimate the position of important anatomic structures such as the carotid artery or cranial nerves, particularly if they are inside the tumor, as in medial peritonal wing meningeomas or transnasal pituitary surgery [50, 191]. The navigation can also help make approaches through the petrosal bone more safe, sparing structures of the inner ear in orofacial approaches to the C2 vertebra [47], and in tumor recurrences at the skull base with a changed anatomic situation. Navigation can be equally applied to drill osseous meningeomas more safely and radically from the skull base [200].

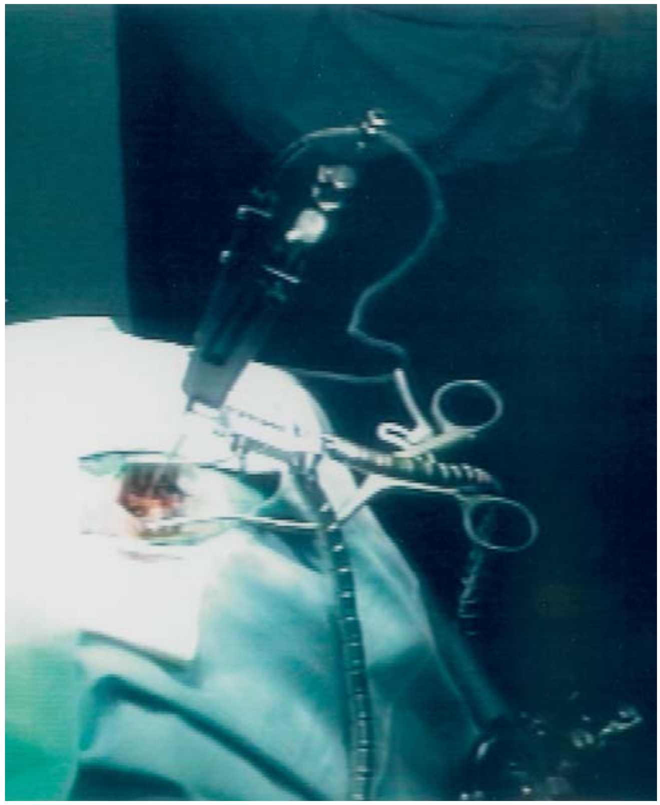

Fig. 14 Navigated stereotactic biopsy with the OTS. The probe holder with the LEDs is fixed by two Leila arms. The Nashold biopsy cannula is introduced through the pointer to the target point

Biopsies

Biopsies can be performed with arm-based and, more easily, with armless pointer systems [20]. For adaptation, the pointer has to be stabilized by a self-retaining retractor attached to the reference arc placed close to the operating field. For this purpose, we use two Laila arms which fix the LED pointer in space (Fig. 14). Using the pointer from the optical tracking system (OTS), the LED holder can be adapted for biopsies by removing the metallic part of the pointer. After registration, the LED holder of the pointer alone is moved in space under optical control on the triplanar reformatted images. Then the pointer is fixed and the cannula introduced through the reducing tubing (the length being identical to that of the removed, metallic pointer). Another adaptation is to use not the pointer but a special probe holder equipped for this purpose with LEDs. Germano [62] reported on 34 biopsies performed successfully with this technique on tumors with diameters of 3.5 cm. Dorward [41] also adapted an optical navigation pointer for biopsies. One advantage over frame-based calculation is the fast finding of a trajectory under visual control and the possibility of radiologic data acquisition before general anesthesia.

Fig. 15 Axial coronal and sagittal CT images of a patient with hydrocephalus during an endoscopically navigated operation. The trajectory through the lateral ventricle and foramen of Monro is visible in all three planes

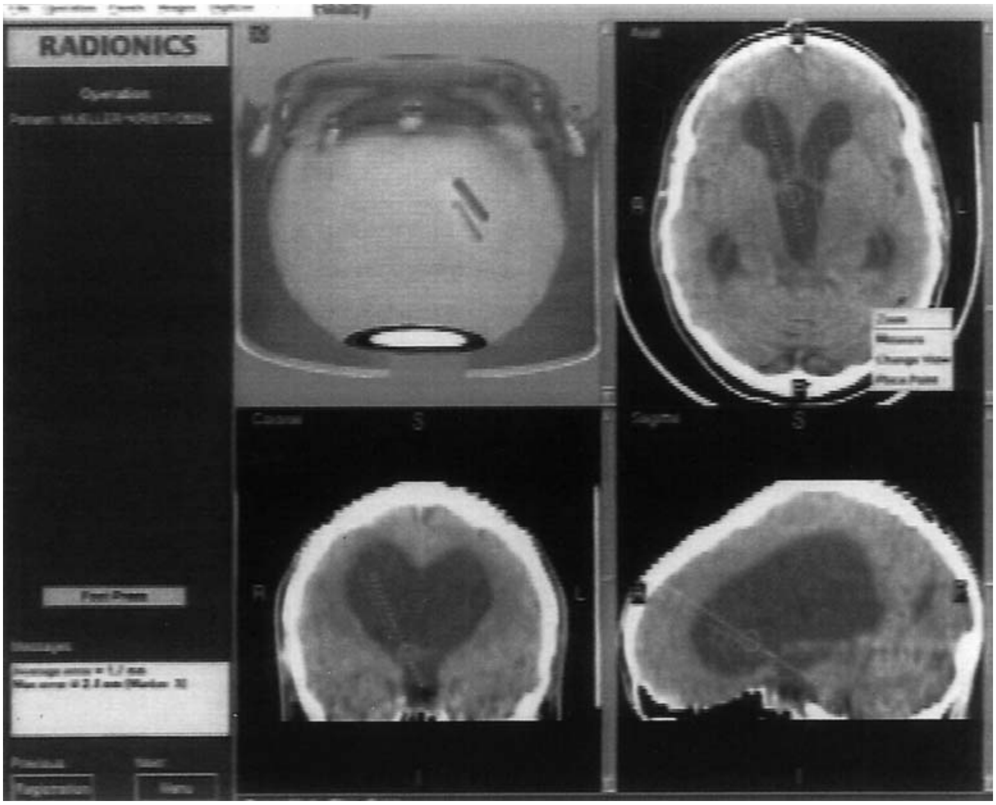

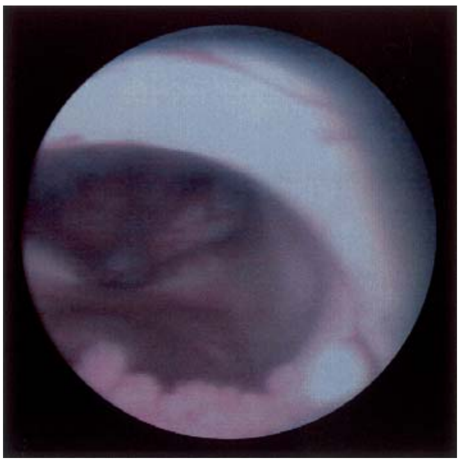

Fig. 16 Endoscopic image of the foramen of Monro with plexus chorioideus and the fornix as the border of the foramen. The view into the third ventricle makes it possible to identify the corpora mammilaria and the adhaesio interthalamica

Endoscopy

Endoscopic procedures are mostly performed by freehand technique [57]. Navigation is however useful in endoscopy if the trajectory has to be planned carefully, for instance in cases of narrow access through the foramen of Monro into the third ventricle to prevent damage to the fornix [77] (Fig. 15, Fig. 16). Either the navigation is performed with the pointer to mark the burr hole and decide the trajectory, or the endoscope itself is used as a pointer navigation system (Fig. 15). In the latter case, an LED array is attached to the endoscope, which is calibrated according to the length of the shaft. Another possibility is to replace the pointer tip by the endoscope and fix it in the LED holder at the appropriate length [39, 99, 169]. Stable fixation by retractors is crucial, because the rigid endoscope with cameras attached is top-heavy and may move, depending on the pivot of the fixation. The application accuracy is low only as long as the ventricles or the cysts are not open. This is also the case when planning the trajectory at the beginning of the procedure.

Inside the third ventricle, Muacevic used navigation in ventriculostomies to fit optimally through the narrow passage of the foramen of Monro [147]. Schröder and Gaab [199] also used navigation in aqueductoplasty to define the best approach to the aqueduct. Navigation is also helpful in cases of biopsies or cysts in the wall of the third ventricle because it gives information about the structures behind the surface of the ventricle wall which are visible by the endoscope. In this way, the best place can be selected for removal of the spacements or perforation point [73].

Above the third ventricle, fenestration of a cavum vergae can be supported by stereotactic methods to plan a trajectory sparing eloquent cortical areas. Also, in cases of very large cysts around the lateral ventricles, the perforation into the lateral ventricle can be cumbersome if the membrane is thick and not translucent. Orientation inside the cyst is difficult if anatomic landmarks are missing. In these cases, navigation helps to find the point of perforation into the lateral ventricle [183]. The endoscopic image itself can be further digitized and mapped into the image space of the navigation system [112]. The spatial assignment allows performance of distance measurements and, theoretically, also coagulation in the presence of bleeding. Zamorano used endoscopic navigation in over 150 tumor cases including biopsies, colloid cyst removals, and tumor extirpations [249].

Procedures close to functionally important cortical areas

The idea of this application is to identify and delineate special functional cortical areas and map this information into the CT/MR images used for navigation [87]. This seems particularly useful for extirpation of lesions close to eloquent cortical or subcortical areas [46].

These cortical areas can be established from conventional CT or MRI using neuroradiologic criteria such as the topography of the sulci, the hump in the gyrus precentralis which represents the hand, the volume of the gyrus precentralis as compared to the thinner gyrus postcentralis, and others. However, in cases of brain edema or cortical displacement by the tumor, localization can be difficult. The classic method of identifying these regions intraoperatively was cortical stimulation. Cushing [32] described in 1909 "a faradic stimulation of the postcentral gyrus in conscious patients." Penfield later used this method in epilepsy surgery [153, 154]. Ojemann [160] applied the stimulation in particular close to speech-relevant areas during ablative epilepsy surgery. Cortical stimulation in the motor strip can be performed under general anesthesia; in speech-relevant areas, the patient has to be awake [215].

Recently, alternative methods were introduced by matching functional information into CT/MR images used for navigation. For the functional mapping, transcranial magnetic stimulation [53, 78], magnetic source imaging [60], MEG [192], and fMRI [18, 31, 59, 78, 102, 115, 116, 132, 187, 202] were used.

Gugino [78] described a transcranial magnetic stimulation device equipped with LEDs which maps the functional information after surface-based registration into appropriate MR images. Using several activation points, the broca region and the gyrus precentralis can be identified. A different approach consists in matching the fMRI images into the CT/MR images performed for navigation. The capacity of MRI to visualize functional activity of the brain was observed first by Belliveau in 1991 [12]. He demonstrated signal changes in the human visual cortex immediately after bolus injection of gadolinium. In 1992, Ogawa [159] described a second imaging technique without contrast medium which detects changes of deoxyhemoglobin as an endogenous contrast medium during cortical activation. Blood flow and the concentration of deoxyhemoglobin in the cerebral capillaries influence the intensity of the MRI signal and reflect indirectly the activity of particular brain areas (the BOLD effect). The main advantage of fMRI over transcranial magnetic stimulation is its capacity to investigate very different brain areas and cognitive functions. Technical problems of fMRI in combination with navigation are:

1. MRI echo planar imaging (EPI) sequences are much more spatially distorted than the common T1 and T2 sequences
2. Movement artefacts must be excluded
3. Only very cooperative patients can be investigated
4. Evaluation of the images is very time-consuming
5. Regarding specificity, very sophisticated psychologic paradigms must be developed

Functional neurosurgery

Intracranial neurosurgical interventions in the deep brain structures regarding pain, extrapyramidal movement disorders, and particularly epilepsy are the classic indications for applying frame-based technique. Nevertheless, navigation can be successfully used in epilepsy surgery for localization and introduction of subdural strip and grid electrodes or for implanting deep-brain electrodes in the hippocampus [150]. Equally interesting is the navigated orientation during ablative surgery in cases of epilepsy, such as with hippocampectomy, to control the resection size [161, 162, 210, 219, 240].

Insertion of catheters

Laborde [118] reported the drainage of abscesses guided by navigation. It is also possible to use these catheters for local antibiotic therapy. Rohde [184] introduced a catheter by navigation into intracranial bleedings for evacuation and lysis therapy. Other authors used the navigated placement of catheters in connection with interstitial radiation therapy [80].

Spinal surgery

Compared to cranial applications, navigation in spinal surgery has some peculiarities regarding anatomy. The spinal cord is much more flexible and therefore dependent on the position of the patient. Skin markers are thus not applicable. Registration must be performed after preparation of the vertebrae on their characteristic anatomic landmarks either with a paired-point technique or in combination with surface matching (Fig. 17, Fig. 18). The dynamic reference frame is fixed on a processus spinosus inside the operating field to register any displacement close to the working space. Tools such as screwdrivers have to be equipped with LED sources. Recently, fluoroscopy could also be integrated into the navigation space [86].

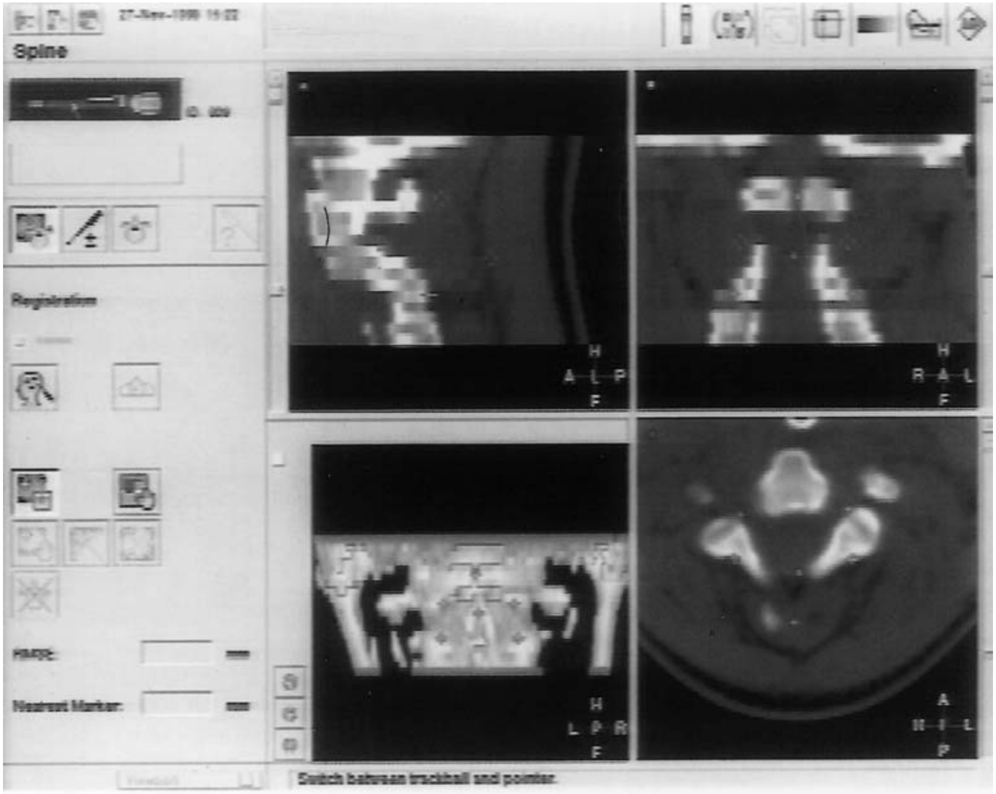

Fig. 17 Intraoperative registration in a spinal procedure using several anatomic bony landmarks

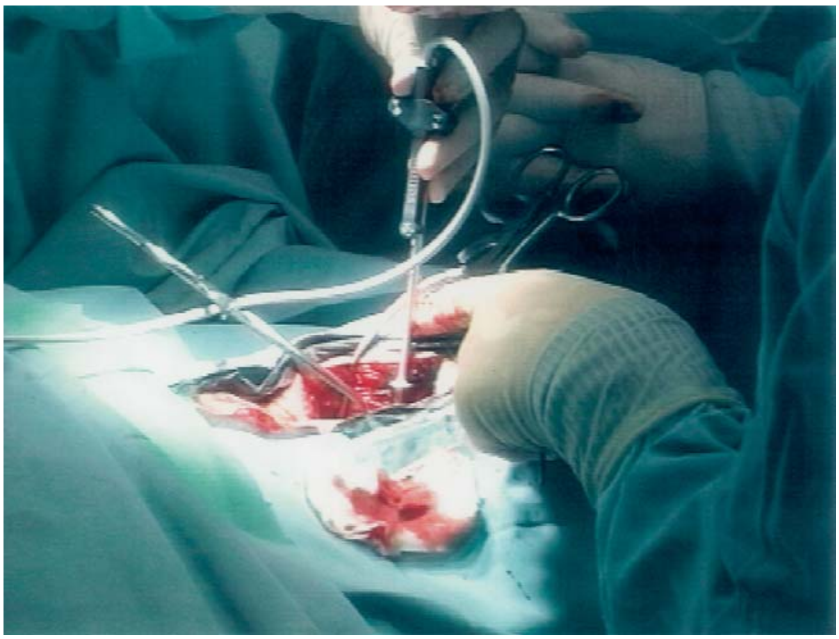

Fig. 18 Intraoperative navigated implantation of screws during a spinal procedure. The screwdriver is equipped with LEDs

Accuracy in spinal applications improved significantly using special spinal navigation technique. In cadaver studies, Glossop [69] found an application accuracy of 2.11±1.49 mm with an angular deviation of 5.11±4.39° using paired-point registration and 2.57±1.34 mm with angular deviation of 4.23±1.84° in combination with surface registration. Merloz [141] measured application accuracy in vivo within 1 mm.

The main clinical indication for computer-aided navigation in spinal surgery is the transpedicular insertion of screws in the thoracolumbar region [16, 17, 25, 68, 141, 149]. Carl [24] showed in cadaver studies that insertion of screws by navigation is more accurate than by fluoroscopy alone. This result was confirmed in vivo by Merloz [141], who observed less than optimal placement of the pedicle screws with navigation in 9% of cases and without navigation in 44%. Navigation was also used in anterior cervical corpectomy [2] to provide better orientation laterally towards the vertebral artery.

Social and economic aspects

Navigation devices are expensive acquisitions for hospitals, with prices in the range of 75,000–250,000 Euros. Therefore it is important to demonstrate their favorable effect on patient outcome and lower operation and hospitalization time. Economic parameters have been investigated concerning duration of operation, hospitalization time, and cost of treatment. Regarding operation time, Alberti [3] found no benefit in navigation for tumor extirpation but significant time savings for stereotactic biopsies. Bingman [14] and Germano [63] showed significantly shorter hospitalization time: for 170 intracranially operated patients with tumor removal, he reported a decrease in stay from 10.8±1.3 days to 7.5±1 days using navigation surgery. For operation of meningeomas, Paleologos [151] found that navigation use reduced patient stay in the hospital from 13.5 days to 8.5 days. Severe complications dropped from 14% to 6% with navigation, and costs per patient were approximately 20% less in this group. Warnick [227] investigated patients with metastasis, including 19 operated on with OTS navigation and 11 in the conventional way. He found no cost reduction by the application of navigation, only reductions in operation time and hospital stay.

Discussion

Stereotactic and microsurgical techniques are accepted methods in contemporary neurosurgery. By means of stereotaxy, straight trajectories and target points are calculated with high accuracy in advance to reach any intracranial point or volume [75, 76]. Microsurgical technique, on the other hand, takes advantage of the imaging modalities to select carefully the approach [154, 155, 156, 157, 189, 241, 242, 243, 244, 245, 246] and reach and extirpate lesions by atraumatic treatment of the tissue with appropriate instruments under microscopic control. Intraoperative orientation in the latter method is based on the surgeon's knowledge of topographic anatomy.

The indications for stereotactic and microsurgical technique have been clearly delineated. When precise determination of a target point was necessary, the stereotactic method was applied, for instance in cases of functional surgery in the basal ganglia and thalamus, in biopsy cases, in interstitial radiation therapy, and for the localization of small tumors. On the other hand, whenever orientation using anatomic structures was sufficient, the microsurgical method was applied exclusively.

With the development of computer-based, navigated surgery, the equilibrium of both techniques seemed to change by the appearance of a third technique somewhere between stereotaxy and microsurgery, claiming to be an accurate stereotactic method and simultaneously a microsurgical technique. This evoked reactions on both sides, fearing loss of competence. The objections of stereotactic neurosurgeons against navigation could be summarized as: Is the expensive navigated method necessary in the presence of much more accurate and consequently better, classic, frame-based stereotaxy?

Microneurosurgeons formulated their hesitations about navigated surgery claiming a future much too dependent on technology. "What happens if the navigation device does not work? Neurosurgeons will lose their skills in finding lesions if they use navigation exclusively for localization." Didactic argument pointed in the same direction: "Young neurosurgeons will not learn classic anatomic localization and then will be unable to operate without the navigation device." Others claim that navigation is only a plaything for neurosurgeons charmed by the magic of high tech. These neurosurgeons argue that intracranial lesions can be found equally successfully without navigation or in difficult cases by means of ultrasound or frame-based stereotaxy.

We would like to deal first with the argument of stereotactically oriented neurosurgeons. It is an error to presume that accuracy is the only criterion of whether a method suits the neurosurgical concept. This assumption is true for stereotactic methodology but not necessarily for microsurgical needs. Microsurgeons require an orientation aid to find lesions atraumatically, but this does not necessarily require subpixel accuracy. It also suits visually oriented microsurgeons to see a target interactively directly in the image space or in the microscope for decisions on craniotomy or direction of the approach and for spatial orientation of his instruments in relation to anatomic structures. They can use the navigation device repeatedly without time-consuming calculation of the coordinates. Furthermore, they are concerned that stereotactic instruments inside the operating field do not restrict their space and view. These qualities are fulfilled by navigated devices and compensate for accuracy loss, which is indeed greater than with frame-based systems.

The tolerable error of the navigation devices depends on the particular application and must be decided during the intervention. An error in the white matter by the navigation device even in the range of 3 mm or 4 mm is still lower than when relying only on neurosurgical knowledge (Fig. 19). Too, if the neurosurgeon is able to calculate the localization and the approach to a small lesion accurately, he feels more confident. The corticotomy is associated with less stress, particularly in functionally important areas such as the central region, if after opening the dura without superficial visible pathology he can confidently approach the right sulcus or make a corticotomy in the correct place just above the lesion by using a navigation device.

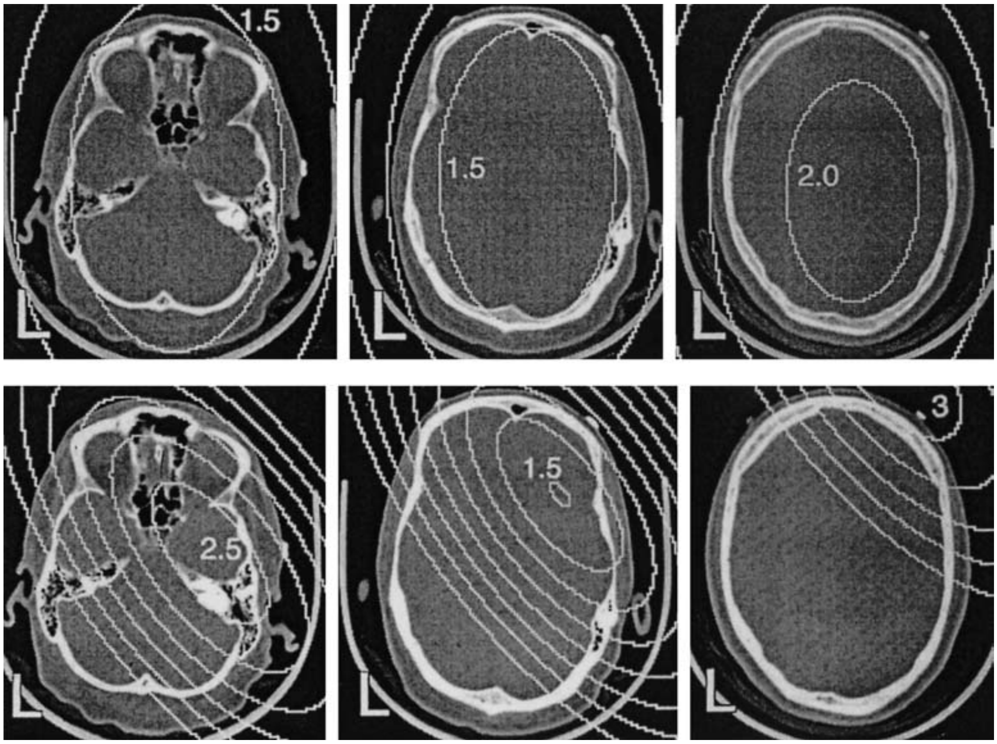

Fig. 19 Computer simulations with different arrangement of the fiducials. The closed lines are places with identical standard deviation. *Top row* The fiducials were arranged optimally around the whole head. The error is very low and does not increase inside the head. *Lower row* The fiducials were placed only in the frontal area. The amplification of the input data error is steep and, particularly in the occipital region, the error is not tolerable

We think Ostertag [163] is right in his reservation toward unreflected enthusiasm for high-tech instruments. The new techniques and instruments have to be at least as successful in mastering practical neurosurgical problems as already established methods. His main argument against navigated surgery deserves additional attention. He aims to show different accuracy for each method and states:

"The navigation method is prone to significant errors as to the intraoperative localization based upon preoperative 3D images. The maximum error can be up to 2.6 cm depending on the extent of the so-called brain shift. In comparison, classic frame-based stereotaxy has a mean error of ±1 mm and remains a gold standard for the exact three-dimensional localization of a given lesion."

In his formulation, Ostertag makes a logical error by comparing the accuracy of both systems under different application modalities. He compares the accuracy of a burr hole procedure with an open craniotomy instead of the accuracy of two stereotactic techniques. It would be more correct to compare the accuracy of both systems for the same type of operation, as in the introduction of a catheter to a target point, for example. Further, if the brain shift, as he states, is the reason for the intraoperative error of navigation, then this error is independent of the stereotactic instrument used and, for frame-based applications during open craniotomy, would also be in the range of 2.6 cm.

Nevertheless, comparing the registration accuracy of frame-based and navigational systems, frame-based calculations are in the range of the image resolution [61, 75, 76, 131], and frameless calculation depends on the method of registration. Using skin markers, the accuracy is in general no better than 2 mm. Under best possible conditions, applying the hybrid method or screws in the skull, the accuracy is also in the range of that with frame-based systems.

The doubts of microneurosurgeons about navigated instruments are in my opinion groundless. The argument of excessive dependence on the navigation and therefore being unable to operate in case the navigation fails is invalid. Navigation instruments are merely tools to improve and simplify some parts of the surgical procedure, not to replace them. Neurosurgeons always have to be able to perform operations without navigation devices. From the didactic point of view, navigation does not interfere negatively with neurosurgical training. On the contrary, we believe that the immediate feedback of spatial information between the pointer tip and the corresponding images much improves the learning effect. Additionally, the stability and robustness of the navigation software is so good that technical failures are extremely rare and usually occur only at the beginning, during the training period.

Another question concerns whether navigation instruments are necessary. Of course neurosurgery was also performed successfully before navigation techniques were developed. This is however not the point. The question is: Can microsurgical technique be *improved* by navigational methods? Someone using a standard big frontal craniotomy for a small meningeoma does not require navigation because the tumor will be inside his operating field anyway. The big standard approaches go back to the time of angiographic localization, where lesions could sometimes be related only to the frontal, temporal, or occipital lobe, depending on the characteristic displacement of the arteries in angiography. However, by improved CT/MR imaging, much more precise anatomic localization is possible, and navigation techniques help in the decision on atraumatic openings and approaches.

If we concede that working with navigation is better than working without it, the question regarding necessity remains. A possible alternative is to use frame-based localization in difficult situations instead of expensive navigated devices. Independently of the above arguments about the better ergonomy of navigated instruments, frame-based procedures put restraints on possible approaches. From the mechanical point of view, it is nearly impossible to use subfrontal, subtemporal, suboccipital, or interhemispheric approaches with the frame. Nevertheless, navigation does not completely displace frame-based stereotaxy. The main indications for classic stereotaxy remain very small targets approached along straight trajectories.

It is sometimes difficult to convince people who do not work with navigation instruments about the benefit of this method. They need their own experience during intraoperative applications. However, the facts that discussions on this topic have nearly ceased (similar to the application of microscopy 30 years ago) and most centers use navigation speak in favor of this technology.

The last objection regarding excessive technology in the operating field making it necessary to pay more attention to the instruments than to the surgery is no longer valid. In the meantime, the software of most navigated instruments is simple, the registration itself is not time-consuming, and at least in our department there is no longer the feeling that using navigation comprises a special type of operation. In fact, it is commonly and routinely used during neurosurgical procedures.

It is difficult to give any prognosis for the development and role of navigated surgery in the future. This is because technology in the computer branch is changing so quickly and new developments not based on the standard coordinate transformation can alter the present situation completely. Unconventional navigation application such as holistic superpositions [111] have been proposed. Manwaring [133] reported on a magnetic emitting source fixed directly to the patient's skull, producing a nonlinear magnetic field through the brain. Flexible catheters with a magnetic tip could be introduced along these nonlinear magnetic trajectories to the target point.

Navigational instruments are presently undergoing a process of evolution and natural selection, with many species arising due to different technical realizations. The best will survive. The criteria for selection are simplicity, accuracy of the neurosurgical procedure, and cost effectiveness. Although we cannot predict future developments, we can already state that navigation reduces risks and hazards during operation and hinders neurosurgical interventions from resembling Odysseus' adventurous wandering on the long journey home from Troy to Ithaca.

References

1. Adams L, Krybus W, Meyer-Ebrecht D, Rüger R, Gilsbach JM, Mösges R, Schlöndorff G (1990) Computer assisted surgery. IEEE Computer Graphics Appl 10:43
2. Albert TJ, Klein GR, Vaccaro AR (1999) Image-guided anterior cervical corpectomy. A feasible study. Spine 15:826–830
3. Alberti O, Dorward NL, Kitchen ND, Thomas DGT (1997) Neuronavigation—impact on operating time. Stereotact Funct Neurosurg 68:44–48
4. Alexander E III, Moriarty TM, Kikinis R, Black P, Jolesz FM (1997) The present and future role of intraoperative MRI in neurosurgical procedures. Stereotact Funct Neurosurg 68:10–17
5. Altuchow NW (1891) Encephalometric investigation of brain in connection with sex, age and cranium size. Publisher unknown, Moscow
6. Apuzzo ML, Chen JC (1999) Stereotaxy, navigation and the temporal concatenation. Stereotact Funct Neurosurg 72:82–88
7. Apuzzo Ml, Sabshin JK (1983) Computed tomographic guidance stereotaxis in the management of the intracranial mass lesions. Neurosurgery 12:277–284
8. Barnett GH, Kormos DW, Steiner CP, Weisenberger J (1993) Intraoperative localization using an armless, frameless stereotactic wand. J Neurosurg 78:510–514
9. Barnett GH, Miller DW (1998) Brain biopsy and related procedures. In: Roberts DW, Barnett GH, Maciunas RJ (eds) Image-guided neurosurgery. Quality Medical, St. Louis, pp 181–191
10. Barnett GH (1996) Surgical management of convexity and falcine meningeomas using interactive image-guided surgery systems. Neurosurg Clin N Am 7:279–284
11. Barnett GH, Steiner CP, Roberts DW (1998) Surgical navigation system technologies. In: Roberts DW, Barnett GH, Maciunas RJ (eds) Image-guided neurosurgery. Quality Medical, St. Louis, pp 17–32
12. Belliveau JW, Kennedy DN, McKinstry RC (1991) Functional mapping of the human visual cortex by magnetic resonance imaging. Science 254:716–719
13. Benabid A, Lavallee S, Hoffmann D, Cinquin P, Demongeot J, Danel F (1992) Computer-driven robot for stereotactic neurosurgery. Computers in stereotactic surgery. Blackwell Scientific, Boston, pp 330–342
14. Bingaman WE, Barnett GH (1998) Social and economic impact of surgical navigation systems. In: Roberts DW, Barnett GH, Maciunas RJ (eds) Image-guided surgery. Quality Medical, St. Louis, pp 231–249
15. Boecher-Schwarz HG, Grunert P, Guenthner M, Kessel G, Mueller-Forell W (1996) Stereotactically guided cavernous malformation surgery. Minim Invas Neurosurg 39:50–55
16. Bolger C, Wigfield C, Melkent T, Smith K (1999) Frameless stereotaxy and anterior cervical surgery. Comput Aided Surg 4:322–327
17. Bolger C, Wigfield C (2000) Image-guided surgery: applications to the cervical and thoracic spine and review of the first 120 procedures. J Neurosurg 92:175–180
18. Boroojerdi B, Folys H, Krings T, Spetzger U, Thron A, Topper R (1999) Localization of the motor hand area using transcranial magnetic stimulation and functional magnetic resonance imaging. Clin Neurophysiol 110:699–704
19. Brinker T, Arango G, Kaminsky S, Samii A, Thorns U, Vorkapic P, Samii M (1998) An experimental approach to image guided skull base surgery employing a microscope based neuronavigation system. Acta Neurochir (Wien) 140:883–889
20. Brommeland T, Henning R (2000) A new procedure for frameless computer navigated stereotaxy. Acta Neurochir (Wien) 142:443–447 21.
Bucholz R, Marzouk S, Levy A (1999) Image guidance and the operating microscope: stealth and neural navigation. In: Alexander E III, Maciunas RJ (eds) Advanced neurosurgical navigation. Thieme, New York, pp 345–355

22. Bucholz R, Macneil WR, Henderson J (1997) Anatomical surface contour matching for efficient registration in image guided neurosurgery. In: Lemke HU, Vannier MW, Inamura K (eds) CAR 97. Elsevier, Amsterdam, pp 772–777
23. Capek K (1931) Rossum's universal robots [Czech]. Aventinum Praha X. Vydani
24. Carl AL, Khanuja HS, Sachs BL, Gatto CA, vom Lehm S, Vosburg K, Schenck J (1997) In vitro simulation. Early results of stereotaxy for pedicle screw placement. Spine 22:1160–1164
25. Carl AL, Khanuja HS, Gatto CA, Matsumoto M, vom Lehm J, Schenck J, Rohling K, Lorensen W, Vosburg K (2000) In vivo pedicle screw placement: image-guided virtual vision. J Spinal Disord 13:225–229
26. Carrau RL, Snyderman CH, Curin HD, Janecka IP, Stechison M, Weissman JL (1996) Computer-assisted intraoperative navigation during skull base surgery. Am J Otolaryng 17:95–101
27. Clarke R (1906) On a method of investigating the deep ganglia and tracts of the central nervous system. Br Med J 2:1799–1800
28. Cormack AM (1963) Representation of a function by its line integrals, with some radiological applications. J Appl Phys 34:2722–2727
29. Cormack AM (1964) Representation of a function by its line integrals with some radiological applications II. J Appl Phys 35:195–207
30. Coste E, Rousseau J, Gibon D, Deleume JF, Blond S, Marchandise X (1993) Frameless method of stereotactic localization with DSA. Neuroradiology 189:829–834
31. Cosgrove GR, Buchbinder BR, Jiang H (1999) Functional magnetic resonance imaging for planning cortical resections. Thieme, New York, pp 201–207
32. Cushing H (1909) A note on the faradic stimulation of the postcentral gyrus in conscious patients. Brain 32:44–53
33. Dandy WE (1918) Ventriculography following the injection of air into the cerebral ventricles. Ann Surg 68:5–12
34. Darabi K, Grunert P, Perneczky A (1997) Accuracy of intraoperative navigation using skin markers. In: Lemke HU, Vannier MW, Inamura K (eds) CAR 97. Elsevier, Amsterdam, pp 920–924
35. David NE (1999) Ergebnisse der rahmenbasierten und rahmenlosen intraoperativen Lokalisation von Gehirnprozessen unter besonderer Berücksichtigung des klinischen Outcomes. Inaugural Dissertation, Mainz
36. Dean D, Kamath J, Duerk JL, Ganz E (1998) Validation of object-induced MR distortion correction for frameless stereotactic neurosurgery. IEEE Trans Med Imaging 17:810–816
37. Denavit J, Hartenberg RS (1955) A kinematic notation for lower-pair mechanisms based on matrices. ASME J Appl Mechanics 22:215–221
38. Descartes R (1984) Passions de l'âme. Meiner, Hamburg
39. Dorward NL, Alberti O, Zhao J, Dijkstra A, Buurman J, Palmer JD, Hawkes D, Thomas DGT (1998) Interactive image-guided neuroendoscopy: development and early clinical experience. Minim Invasive Neurosurg 41:31–34
40. Dorward NL, Alberti O, Velani B, Gertsen FA, Harkness WF, Kitchen ND, Thomas DGT (1998) Postimaging brain distortion: magnitude, correlates, and impact on neuronavigation. J Neurosurg 88:656–662
41. Dorward NL, Alberti O, Palmer JD, Kitchen ND, Thomas DGT (1999) Accuracy of true frameless stereotaxy: in vivo measurement and laboratory phantom studies. Technical note. J Neurosurg 90:160–168
42. Doshi PK, Lemmieux L, Fish DR, Shorvon SD, Harkness WH, Thomas DGT (1995) Frameless stereotaxy and interactive neurosurgery with the ISG viewing wand. Acta Neurochir Suppl (Wien) 64:49–53
43. Drake JM, Joy M, Goldenberg A, Kreindler D (1991) Computer-and robot-assisted resection of thalamic astrocytomas in children. Neurosurgery 29:27–33
44. Drake JM, Rutka JT, Hoffmann HJ (1994) ISG viewing wand. Neurosurgery 34:1094–1097
45. Drake JM, Prudencio J, Holowaka S, Rutka JT, Hoffmann HJ, Humphrey RP (1994) Frameless stereotaxy in children. Pediatr Neurosurg 20:152–159
46. Duffau H (2000) Intraoperative direct subcortical stimulation for identification of the internal capsule, combined with an image-guided stereotactic system during surgery for basal ganglia lesions. Surg Neurol 53:250–254
47. Dyer PV, Patel N, Pell GM, Cumminis B, Sandeman DR (1995) The ISG viewing wand: an application to atlanto-axial cervical surgery using the Le Fort I maxillary osteotomy. Br J Oral Maxillofac Surg 33:370–374
48. Ebeling U, Hasdemir MG, Barth A (1993) Stereotaktisch geleitete Mikrochirurgie zerebraler Prozesse. Schweiz Med Wochenschr 123:1585–1590
49. Ebeling U, Steinmetz H, Huang Y, Kahn T (1989) Topography and identification of the inferior precentral sulcus in MR image. AJNR 10:937–942
50. Elias WJ, Chadduck JB, Alden TD, Laws ER Jr (1999) Frameless stereotaxy for transsphenoidal surgery. Neurosurgery 45:271–275
51. Ende G, Treuer H, Boesecke R (1992) Optimization and evaluation of landmark-based image correlation. Phys Med Biol 37:261–271
52. El Jamel MS (1997) Accuracy, efficacy, and clinical applications of the radionics operating arm system. Comput Aid Surg 2:292–297
53. Ettinger GJ, Grimson WEL, Leventon ME (1996) Noninvasive functional brain mapping using registered transcranial magnetic stimulation. Proceedings of the IEEE workshop on mathematical methods in biomedical image analysis, San Francisco, pp 21–22
54. Fleig OJ, Edwards PJ, Chandra S, Süttler H, Hawkes DJ (1998) Automated microscope calibration for image guided surgery. In: Lemke HU, Vannier MW, Inamura K, Farman A (eds) CAR 98. Elsevier, Amsterdam, pp 747–752
55. Forstad H, Hariz M, Ljunggren B (1991) History of Clare's stereotactic instrument. Stereotact Funct Neurosurg 57:130–140
56. Fankhauser H, Glauser D, Flury P, Piguet Y, Epitaux M, Favre J, Meuli RA (1994) Robot for CT-guided stereotactic neurosurgery. Stereotact Funct Neurosurg 63:93–98
57. Fries G, Perneczky A (1999) Intracranial endoscopy. In: Cohadon F (ed) Advances and technical standards in neurosurgery, vol 25. Springer, Vienna, pp 21–60
58. Friets EM, Strobehn JW, Hatch JF, Roberts DW (1989) A frameless stereotactic operating microscope for neurosurgery. IEEE Trans Biomed Eng 36:608–617
59. Gallen CC, Tecoma E, Iragui V, Sobel DF, Schwartz BJ, Bloom FE (1997) Magnetic source imaging of abnormal low frequency magnetic activity in presurgical evaluation of epilepsy. Epilepsia 38:452–460
60. Gallen CC, Schwartz BJ, Bucholz RD, Malik G, Barkley GL, Smith J, Tung H, Copeland B, Bruno L, Assam S, Hirschkoff E, Bloom F (1995) Presurgical localization of functional cortex using magnetic source imaging. J Neurosurg 82:988–994
61. Galloway RL, Maciunas RJ, Edwards CA (1992) Interactive image-guided neurosurgery. IEEE Trans Biomed Eng 39:1226–1231
62. Germano IM, Queenan JV (1998) Clinical experience with intracranial needle biopsy using frameless surgical navigation. Comput Aided Surg 3:33–39
63. Germano IM, Villalobos H, Silvers A, Post KD (1999) Clinical use of the optical digitizer for intracranial neuronavigation. Neurosurgery 45:261–269
64. Gildenberg PL (1997) The history of stereotactic and functional neurosurgery. In: Gildenberg PL, Tasker RR (eds) Textbook of stereotactic and functional neurosurgery. McGraw-Hill, New York, pp 1–15
65. Giorgi C, Eisenberg H, Costi G, Gallo E, Garibotto G, Casolino D (1995) A robot assisted microscope for neurosurgery. Proceedings of MRCAS, pp 334–339

66. Giorgi C, Casolino DS (1997) Preliminary clinical experience with intraoperative stereotactic ultrasound imaging. Stereotact Funct Neurosurg 68:54–58
67. Glauser D, Fankhauser H, Epitaux M, Hefti JL, Jaccottet A (1995) Neurosurgical robot minerva: first results and current developments. J Image Guid Surg 1:266–272
68. Glossop N, Hu R (1997) Effect of registration method on clinical accuracy of image guided pedicle screw surgery. In: Lemke HU, Vannier MW, Inamura K (eds) CAR 97. Elsevier, Amsterdam, pp 884–888
69. Glossop N, Hu R (1997) Clinical use accuracy in image guided surgery. In: Lemke HU, Vannier MW, Inamura K (eds) CAR 97. Elsevier, Amsterdam, pp 889–893
70. Goertz RC (1963) Manipulators used for handling radioactive materials. In: Benett EM (ed) Human factors in technology. McGraw-Hill, New York
71. Golfinos JG, Fitzpatrick BC, Smith LR, Spetzler RF (1996) Clinical use of a frameless stereotactic arm: results of 325 cases. J Neurosurg 83:287–292
72. Grimson WEL, Ettinger GJ, White SJ, Lozano-Perez T, Wells WM III, Kikinis R (1996) An automatic registration method for frameless stereotaxy, image guided surgery and enhanced reality visualization. IEEE Trans Med Imaging 5:129–140
73. Grunert P, Hopf N, Perneczky A (1997) Framebased and frameless endoscopic procedures in the third ventricle. Stereotact Funct Neurosurg 68:80–89
74. Grunert P, Mueller-Forell W, Darabi K, Reisch R, Busert C, Hopf N, Perneczky A (1998) Basic principles and clinical applications of neuronavigation and intraoperative computed tomography. Comput Aid Surg 3:166–173
75. Grunert P, Mäurer J, Müller-Forell W (1999) Accuracy of stereotactic coordinate transformation using a localization frame and computed tomographic imaging. Part I. Influence of the mathematical and physical properties of the CT on the image of the rods of the localization frame and the determination of their centres. Neurosurg Rev 22:173–187
76. Grunert P (1999) Accuracy of stereotactic coordinate transformation using a localization frame and computed tomographic imaging. Part II. Analysis of matrix-based coordinate transformation. Neurosurg Rev 22:188–203
77. Grunert P, Perneczky A, Resch K (1994) Endoscopic procedures through the foramen of Monro under stereotactic conditions. Minim Invas Neurosurg 37:2–8
78. Gugino LD, Potts GF, Aglio LS, Alexander E III, Grimson WEL, Kikinis R, Shenton M, Black P, Ettinger GJ, Coste WA, Leventon M, Gonzalez AA (1999) Localization of eloquent cortex using transcranial magnetic stimulation. In: Alexander E III, Maciunas RJ (eds) Advanced neurosurgical navigation. Thieme, New York, pp 163–199
79. Gumprecht HK, Widenka DC, Lumenta CB (1999) BrainLab vectorvision neuronavigation system: technology and clinical experience in 131 cases. Neurosurgery 44:97–104
80. Gunkel AR, Freysinger W, Hensler E, Auer T, Eichinger P, Auberger T, Bale RJ, Vogele M, Martin A, Thumfart WF, Lukas P (1997) Computer assisted stereotactic frameless interstitial brachytherapy. In: Lemke HU, Vannier MW, Inamura K (eds) CAR 97. Elsevier, Amsterdam, pp 404–409
81. Guthrie BL (1994) Graphic-interactive cranial surgery: the operating arm system. In: Pell MF, Thomas DGT (eds) Handbook of stereotaxy using the CRW apparatus. Williams and Wilkins, Baltimore, pp 193–210
82. Guthrie BL, Adler JR (1992) Computer-assisted preoperative planning, interactive surgery and frameless stereotaxy. Clin Neurosurg 38:112–131
83. Guthrie BL (1998) Cerebral metastatic disease. In: Roberts DW, Barnet GH, Maciunas RJ (eds) Image guided neurosurgery. Quality Medical, St. Louis, pp 73–76
84. Haase J (1999) Image-guided neurosurgery/neuronavigation/the surgiscope. Reflections on a theme. Minim Invasive Neurosurg 42:53–59
85. Haase J (1999) Neuronavigation. Childs Nerv Syst 15:755–777
86. Hamadeh A, Lavallee S, Cinquin P (1998) Automated 3-dimensional computed tomographic and fluoroscopic image registration. Comput Aided Surg 3:11–19
87. Hamilton R, Sweeney P, Pelizzari C, Yetkin F, Holman B, Garada B, Weichselbaum R, Chen G (1997) Functional imaging in treatment planning of brain lesions. Int J Radiol Oncol Biol Phys 37:181–188
88. Hardenack M, Bucher N, Falk A, Harders A (1998) Preoperative and intraoperative navigation: status quo and perspectives. Comput Aided Surg 3:153–158
89. Hassfeld S, Zoller J, Albert FK, Wirtz CR, Knauth M, Muhling J (1998) Preoperative planning and intraoperative navigation in skullbase surgery. J Craniomaxillofac Surg 26:220–225
90. Hata N, Dohi T, Iseki H, Takakura K (1997) Development of a frameless and armless stereotactic neuronavigation system with ultrasonographic registration. Neurosurgery 41:608–613
91. Hauser R, Westermann B, Probst R (1997) Non-invasive tracking of patients' head movements during computer-assisted intranasal microscopic surgery. Laryngoscope 107:491–499
92. Hauser R, Westermann B, Probst R (1997) A noninvasive patient registration and reference system for interactive intraoperative sinus surgery. Proc Inst Mech Eng 211:327–334
93. Heilbrun MP (1984) Computed tomography-guided stereotactic system. Clin Neurosurg 31:564–581
94. Heilbrun MP, McDonald P, Wiker C (1992) Stereotactic localization and guidance using a machine vision technique. Stereotact Funct Neurosurg 58:94–98
95. Helm PA, Eckel T (1998) Accuracy of registration methods in frameless stereotaxis. Comput Aided Surg 3:51–56
96. Henderson JM, Smith KR, Bucholz RD (1994) An accurate and ergonomic method for registration for image-guided surgery. Comput Med Imaging Graph 18:273–277
97. Homer (1974) Iliad. Murray AT (ed) Harvard University Press, London
98. Homer (1974) Odyssey. Murray AT (ed) Harvard University Press, London
99. Hopf NJ, Grunert P, Darabi K, Busert C, Bettag M (1999) Frameless neuronavigation applied to endoscopic neurosurgery. Minim Invasive Neurosurg 42:187–193
100. Horsley V, Clarke RH (1908) The structure and functions of the cerebellum examined by a new method. Brain 31:45–124
101. Horstmann GA, Reinhardt HF (1994) Ranging accuracy test of the sonic microstereotactic system. Neurosurgery 34:754–755
102. Hounsfield GN (1973) Computerized transaxial scanning (tomography). Part I: Description of a system. Br J Radiol 46:1016–1022
103. Hunnerup PB, Nielsen JB (1994) Real time navigation. System for neurosurgery. Master's thesis. Aalborg University, Denmark
104. Kai J, Shiomi H, Sasama T, Sato Y, Inoue T, Tamura S (1998) An optical high-precision 3-D position measurement system suitable for head motion tracking in frameless stereotactic radiosurgery. In: Lemke HU, Vannier MW, Inamura K, Farman A (eds) CAR 98. Elsevier, Amsterdam, pp 599–604
105. Kato A, Yoshimine T, Hayakawa T, Tomita Y, Ikeda T, Mitomo M, Harada K, Mogami H (1991) A frameless, armless navigation system for computer-assisted neurosurgery. J Neurosurg 74:845–849
106. Kelly PJ (1999) Electromagnetic operative guidance: the regulus navigator. In: Alexander E III, Maciunas RJ (eds) Advanced neurosurgical navigation. Thieme, New York, pp 365–372
107. Kelly PJ, Kall B, Goerss S (1984) Transposition of volumetric information derived from CT scanning in stereotactic space. Surg Neurol 21:465–471
108. Kirschner M (1933) Die Punktionstechnik und die Elektrokoagulation des Ganglion Gasseri. Über gezielte Operationen. Arch Klin Chir 176:581–620

109. Kiya N, Dureca C, Fukushima T, Maroon JC (1997) Computer navigational microscope for minimally invasive neurosurgery. Minim Invasive Neurosurg 40:110–115
110. Knauth M, Wirtz CR, Tronnier VM, Staubert A, Kunze S, Sartor K (1998) Intraoperative magnetic resonance tomography for control of extent of neurosurgical operations. Radiologe 38:218–224
111. Ko K (1998) Superimposed holographic image-guided neurosurgery. Technical note. J Neurosurg 88:777–781
112. Konen W, Scholz M, Tombrock S (1998) The VN project: endoscopic image processing for neurosurgery. Comput Aided Surg 3:144–148
113. Kosugi Y, Watanabe E, Goto J (1988) An articulated neurosurgical navigation system using MRI and CT images. IEEE Trans Biomed Eng 35:147–152
114. Koivukangas J, Louhisalmi Y, Alakuijala J, et al (1993) Ultrasound-controlled neuronavigator-guided brain surgery. J Neurosurg 79:36–42
115. Krings T, Reul J, Spetzger U, Klusmann A, Roessler F, Gilsbach JM, Thron A (1998) Functional magnetic resonance mapping of sensory motor cortex for image-guided neurosurgical intervention. Acta Neurochir (Wien) 140:215–222
116. Krombach GA, Spetzger U, Rohde V, Gilsbach JM (1998) Intraoperative localization of functional regions in the sensomotor cortex by neuronavigation and cortical mapping. Comput Aided Surg 3:64–73
117. Kwoh YS, Hou J, Jonckheere EA, Hayati S (1988) A robot with improved absolute positioning accuracy for CT guided stereotactic brain surgery. IEEE Trans Biomed Eng 35:153–160
118. Laborde G, Klimek L, Harders A, Gilsbach J (1993) Frameless stereotactic drainage of intracranial abscesses. Surg Neurol 40:16–21
119. Lavallee S (1996) Registration for computer-integrated surgery: methodology, state of the art. In: Taylor RH, Lavallee S, Burdea GC, Mösges R (eds) Computer-integrated surgery. MIT Press, Cambridge, pp 77–97
120. Lavallee S, Szelisky R, Brunie L (1996) Anatomy-based registration of three-dimensional medical images, range images, X-ray projections, and three-dimensional models using octree-splines. In: Taylor RH, Lavallee S, Burdea GC, Mösges R (eds) Computer-integrated surgery. MIT Press, Cambridge, pp 115–143
121. Lawton MT, Spetzler RF (1999) Clinical experience with a frameless stereotactic arm in intracranial neurosurgery. In: Alexander E III, Maciunas RJ (eds) Advanced neurosurgical navigation. Thieme, New York, pp 321–332
122. Leksell L (1949) A stereotactic apparatus for intracranial surgery. Acta Chir Scand 99:229–233
123. Leksell L (1951) The stereotactic method and radiosurgery of the brain. Acta Chir Scand 102:316–319
124. Lewis JT, Galloway RL Jr, Schreiner S (1998) An ultrasound approach to localization of fiducial markers for interactive, image-guided neurosurgery. Part I: Principles. IEEE Trans Biomed Eng 45:620–630
125. Longerich UJ, Carls FR, Broennimann R, Sailer HF (1997) The accuracy of the virtual patient system for cranio-maxillofacial navigation. In: Lemke HU, Vannier MW, Inamura K (eds) CAR 97. Elsevier, Amsterdam, pp 729–732
126. Luber J, Mackevics A (1995) Multiple coordinate manipulator (MKM). A computer assisted microscope. In: Lemke HU, Vannier MW (eds) CAR 95. Elsevier, Amsterdam pp 1121–1125
127. Maciunas RJ, Galloway RL, Fitzpatrick JR, Mandava VR, Edwards CA, Allen GS (1992) A universal system for interactive image-directed neurosurgery. Stereotact Funct Neurosurg 58:108–113
128. Maciunas RJ (1999) Overview of interactive image-guided neurosurgery: principles, applications, and new techniques. In: Alexander E III, Maciunas RJ (eds) Advanced neurosurgical navigation. Thieme, New York, pp 15–32
129. Maciunas RJ, Fitzpatrick JM, Gadamsetty S, Mauer CR Jr (1996) A universal method for geometric correction of magnetic resonance images for stereotactic neurosurgery. Stereotact Funct Neurosurg 66:137–140
130. Maciunas RJ, Berger MS, Copeland B, Mayberg MR, Selker R, Allen GS (1996) A technique for interactive image-guided neurosurgical intervention in primary brain tumors. Neurosurg Clin N Ann 7:245–266
131. Maciunas RJ, Galloway RL, Latimer JW (1994) The application accuracy of stereotactic frames. Neurosurgery 35:682–695
132. Maldijian J, Atlas SW, Howard RS II, Greenstein E, Alsop D, Detre JA, Liesterud J, D'Exposito M, Flamm ES (1996) Functional magnetic resonance imaging of regional brain activity in patients with intracerebral arteriovenous malformations before surgical or endovascular therapy. J Neurosurg 84:477–483
133. Manwaring KH (1999) Neuronavigation using magnetic fields. Workshop on endoscopy and navigation. Greifswald (personal communication)
134. Masamune K, Ji L, Suzuki M, Dohi T, Iseki H, Takakura K (1998) A new development of stereotactic robot with detachable drive for neurosurgery. In: Lemke HU, Vannier MW, Inamura K, Farman A (eds) CAR 98. Elsevier, Amsterdam, pp 664–669
135. Matula C, Roessler K, Reddy M, Schindler E, Koos WT (1998) Intraoperative computed tomography guided neuronavigation: concepts, efficiency, and work flow. Comput Aided Surg 3:174–182
136. Maurer CR, Maciunas RJ, Fitzpatrick JM (1998) Registration of head CT images to physical space using a weighted combination of points and surfaces. IEEE Trans Med Imaging 17:753–761
137. Maurer CR, Aboutanos GB, Dawant BM, Gadamsetty S, Margolin RA, Maciunas RJ (1996) Effect of geometrical distortion correction in MR on image registration accuracy. J Comput Assist Tomogr 20:666–679
138. Maurer CR, Fitzpatrick JM, Wang MY, Galloway RL Jr, Maciunas RJ, Allen GS (1997) Registration of head volume images using implantable fiducial markers. IEEE Trans Med Imaging 16:447–462
139. Mauerer CR, Hill DL, Martin AJ, Liu H, McCue M, Rueckert D, Lloret D, Hall WA, Maxwell RC, Hawkes DJ, Truwit CL (1998) Investigation of intraoperative brain deformation using a 1.5 T interventional MR system. preliminary results. IEEE Trans Med Imaging 17:817–825
140. McDermott MW (1998) Intracranial gliomas. In: Roberts DW, Barnett GH, Maciunas RJ (eds) Image-guided neurosurgery. Quality Medical, St. Louis, pp 77–86
141. Merloz P, Tonetti J, Cinquin P, Lavalles S, Troccaz J, Pitet L (1998) Chirurgie assistée par ordinateur: visage automatisé de pèdicules vertebreaux. Chirurgie 123:482–490
142. Miga MI, Paulsen KD, Lemery JM, Eisner SD, Hartov A, Kennedy FE, Roberts DW (1999) Model-updated image guidance: initial clinical experiences with gravity-induced brain deformation. IEEE Trans Med Imaging 18:866–874
143. Moniz E (1927) L'encephalographie arterielle, s'importance dans la localisation des tumeurs cerebrales. Rev Neurol 2:72–89
144. Mösges R, Schlöndorff G (1988) A new imaging method for intraoperative therapy control in skull base surgery. Neurosurg Rev 11:245–247
145. Mösges R, Lavallee S (1996) Multimodal information for computer-integrated surgery. In: Taylor RH, Lavallee S, Burdea GC, Mösges R (eds) Computer integrated surgery. MIT Press, Cambridge, pp 5–19
146. Muacevic A, Steiger HJ (1999) Computer-assisted resection of cerebral arteriovenous malformations. Neurosurgery 45:1164–1170
147. Muacevic A, Muller A (1999) Image-guided endoscopic ventriculostomy with a new frameless armless neuronavigation system. Comput Aided Surg 4:87–92

148. Nabavi A, Manthei G, Blömer U, Kumpf L, Klinge H, Mehdorn HM (1995) Neuronavigation. Computerunterstütztes Operieren in der Neurochirurgie. Radiologe 35:573–577
149. Nolte LP, Visarius H, Arm E, Langlotz F, Schwarzenbach O, Zamorano L (1995) Computer aided fixation of spinal implants. J Image Guided Surg 1:88–93
150. Nguyen JP, Lefaucher JP, Decq P, Uchiyama T, Carpentier A, Fontaine D, Brugieres P, Pollin B, Feve A, Rostaing S, Cesaro P, Keravel Y (1999) Chronic motor cortex stimulation in the treatment of central and neuropathic pain. Correlation between clinical, electrophysiological and anatomical data. Pain 82:245–251
151. Paleologos TS, Wadley JP, Kitchen ND, Thomas DG (2000) Clinical utility and cost-effectiveness of interactive image-guided craniotomy: clinical comparison between conventional and image-guided meningeoma surgery. Neurosurgery 47:40–47
152. Pelizzari CA, Chen GTY (1987) Registration of multiple diagnostic image scans using surface fitting. In: The use of computers in radiation therapy. Elsevier, Amsterdam, pp 437–440
153. Penfield W, Roberts L (1959) Speech and brain mechanisms. Princeton University Press, Princeton
154. Penfield W, Boldrey E (1937) Somatic motor and sensory representation in the cerebral cortex of man as studied by electrical stimulation. Brain 60:389–443
155. Perneczky A, Fries G (1998) Endoscope-assisted brain surgery. Part I. Evolution, basic concept, and current technique. Neurosurgery 42:219–225
156. Perneczky A, Tschabitscher M, Resch KDM (1993) Endoscopic anatomy for neurosurgery. Thieme, Stuttgart
157. Perneczky A, Müller-Forell W, van Lindert E (1998) Key hole concept in neurosurgery with endoscope-assisted microsurgery. Twenty-five case studies. Thieme, Stuttgart
158. Pieper DL (1968) The kinematics of manipulators under computer control. Standford artificial intelligence laboratory, Standford University AIM 72
159. Ogawa S, Tank DW, Menon R (1992) Intrinsic signal changes accompanying sensory stimulation: functional brain mapping with magnetic resonance imaging. Proc Natl Acad Sci U S A 89:5951–5955
160. Ojeman G, Ojeman J, Lettich E, Berger M (1989) Cortical language localization in left, dominant hemisphere. J Neurosurg 71:316–326
161. Olivier A, Germano IM, Cukiert A, Peters T (1994) frameless stereotaxy for surgery of the epilepsies: preliminary experience. J Neurosurg 81:629–633
162. Olivier A, Cyr M, Comeau R, Peters T, Boling W, Klein D, Reutens D (1999) Image guided surgery of epilepsy and intrinsic brain tumors. In: Alexander E III, Maciunas RJ (eds) Advanced neurosurgical navigation. Thieme, New York, pp 469–482
163. Ostertag CB, Warnke PC (1999) Neuronavigation. Computerassistierte Neurochirurgie. Nervenarzt 70:517–521
164. Radon J (1917) Über die Bestimmung von Functionen durch ihre Integralwerte längs gewisser Mannigfaltigkeiten. Berichte Sächsischer Akademie der Wissenschaften. Leipzig Math-Phys Kl 69:262–277
165. Reinges MH, Spetzger U, Rohde V, Adams L, Gilsbach JM (1998) Experience with a new multifunctional articulated instrument holder in minimally invasive navigated surgery. Minim Invas Neurosurg 41:149–151
166. Reinhardt HF, Meyer H, Amrein E (1988) A computer-assisted device for intraoperative CT-correlated localization of brain tumors. Eur Surg Res 20:51–58
167. Reinhardt HF, Horstmann GA, Gratzl O (1993) Sonic stereometry in microsurgical procedures for deep-seated brain tumors and vascular malformations. Neurosurgery 32:51–57
168. Reinhardt HF, Trippl M, Westermann B, Horstmann GA, Gratzl O (1996) Computer assisted brain surgery for small lesions in the central sensorimotor region. Acta Neurochir (Wien) 138:200–205
169. Rhoten RL, Luciano MG, Barnett GH (1997) Computer-assisted endoscopy for neurosurgical procedures: technical note. Neurosurgery 40:632–637
170. Riechert T, Wolff M (1952) Ein neues Zielgerät für die Koagulation des Ganglion Gasseri und andere intracerebrale Eingriffe. Acta Neurochir 2:405–407
171. Roberts LG (1963) Machine perception of three-dimensional Solids. Lincoln Laboratory, Massachusetts Institute of Technology report no. 315
172. Roberts LG (1965) Homogenous matrix representation and manipulation of N-dimensional constructs. Lincoln Laboratory, Massachusetts Institute of Technology document no. MS1045
173. Roberts DW (1999) Stereotactic guidance with the operating microscope: surgiscope. In: Alexander E III, Maciunas RJ (eds) Advanced neurosurgical navigation. Thieme, New York, pp 333–343
174. Roberts DW, Miga MI, Hartov A, Eisner S, Lemery JM, Kennedy FE, Paulsen KD (1999) Intraoperatively updated neuroimaging using brain modeling and sparse data. Neurosurgery 45:1199–1206
175. Roessler K, Ungersboeck K, Dietrich W, Aichholzer M, Hittmeir K, Matula C, Czech T, Koos WT (1997) Frameless stereotactic guided neurosurgery: clinical experience with an infrared based pointer device navigation system. Acta Neurochir (Wien) 139:551–559
176. Roessler K, Ungersboeck K, Czech T, Aichholzer M, Dietrich W, Goerzer H, Matula C, Koos WT (1997) Contour-guided brain tumor surgery using a stereotactic navigation microscope. Stereotact Funct Neurosurg 68:33–38
177. Roessler K, Ungersboeck K, Aichholzer M, Dietrich W, Czech T, Heimberger K, Matula C, Koos WT (1998) Image-guided neurosurgery comparing a pointer device system with a navigating microscope: a retrospective analysis of 208 cases. Minim Invasive Neurosurg 41:53–57
178. Roessler K, Ungersboeck K, Aichholzer M, Dietrich W, Goerzer H, Matula C, Czech T, Koos WT (1998) Frameless stereotactic lesion contour-guided surgery using a computer-navigated microscope. Surg Neurol 49:282–288
179. Roessler K, Czech T, Dietrich W, Ungersboeck K, Nasel C, Hainfellner JA, Koos WT (1998) Frameless stereotactic-directed tissue sampling during surgery of suspected low-grade gliomas to avoid histological undergrading. Minim Invasive Neurosurg 41:183–186
180. Roberts DW, Hartov A, Kennedy FE, Miga MI, Paulsen KD (1998) Intraoperative brain shift and deformation: a quantitative analysis of cortical displacement in 28 cases. Neurosurgery 43:749–760
181. Roberts DW, Nakayama T, Brodwater BK; Pavlidis J, Friets EM, Fagan E, Hartov A, Strohbehn JW (1992) Further development and clinical application of the stereotactic operating microscope. Stereotact Funct Neurosurg 58:114–117
182. Roberts DW (1998) Fundamentals of registration. In: Roberts DW, Barnett GH, Maciunas RJ (eds) Image-guided neurosurgery. Quality Medical, St. Louis, pp 1–15
183. Rohde V, Reinges MH, Krombach GA, Gilsbach JM (1998) The combined use of image-guided frameless stereotaxy and neuroendoscopy for the surgical management of occlusive hydrocephalus and intracranial cysts. Br J Neurosurg 12:531–538
184. Rohde V, Rohde I, Reinges MH, Mayfrank L, Gilsbach JM (2000) Frameless stereotactically guided catheter placement and fibrinolytic therapy for spontaneous intracerebral hematomas: technical aspects and initial clinical results. Minim Invasive Neurosurg 43:9–17
185. Rosenberg J (1972) A history of numerical control 1949–1972. The technical development, transfer to industry, and assimilation. Report no. ISI-RR-72–3. USC Information Sciences Institute, Marina del Rey
186. Rousseau J, Gibon D, Coste E, Blond S, Pertuzon B, Coche B, Vasseur C, Marchandise X (1995) A frameless stereotactic

localization system using MRI, CT, and DSA. Acta Neurochir Suppl (Wien) 64:40–44
187. Roux FE, Ranjeva JP, Boulanouar K, Manelfe C, Sabatier J, Tremoulet M, Berry I (1997) Motor functional MRI for presurgical evaluation of cerebral tumors. Stereotactic Funct Neurosurg 68:106–111
188. Ryan MJ, Erickson RK, Levin DN, Pelizzari CA, Macdonald RL, Dohrmann GJ (1996) Frameless stereotaxy with real time tracking of patient's head movement and retrospective patient-image registration. J Neurosurg 85:287–292
189. Samii M, Carvalho GA, Tatagiba M, Matthies C, Vorkapic P (1996) Meningeomas of the tentorial notch: surgical anatomy and management. J Neurosurg 84:375–381
190. Sandeman DR, Gill SS (1995) The impact of interactive image guided surgery: the Bristol experience with the ISG/Elekta viewing wand. Acta Neurochir Suppl 64:54–58
191. Sandeman D, Moufild A (1998) Interactive image-guided pituitary surgery. An experience of 101 procedures. Neurochirurgie 44:331–338
192. Scarabin JM, Jannin P, Schartz D, Morandi X. MEG and 3-D navigation in image guided neurosurgery. In: Lemke HU, Vannier MW, Inamura K (eds) CAR 97. Elsevier, Amsterdam pp 767–771
193. Scheinmann VD (1969) Design of a computer manipulator. Standford artificial intelligence laboratory. Standford University, AIM 92
194. Schmerber S, Chen B, Lavallee S, Chirosel JP, Poyet A, Colomb M, Reyt E (1997) Markerless hybrid registration method for computer assisted endoscopic ENT surgery. In: Lemke HU, Vannier MW, Inamura K (eds) CAR 97. Elsevier, Amsterdam pp 799–806
195. Schmieder K, Hardenack M, Harders A (1998) Neuronavigation in daily routine of a neurosurgical department. Comput Aided Surg 3:159–161
196. Schleidt DT, Dobrzeniecky AB, Dirksen KL, Larsen P, Kreiborg S (1998) Volume imaging for maxillofacial applications: estimation and analysis of CT measurement errors. In: Lemke HU, Vannier MW, Inamura K, Farman A (eds) CAR 98. Elsevier, Amsterdam, pp 773–779
197. Schlöndorff G, Meyer-Ebrecht D, Mösges R, Krybus W, Adams L (1987) CAS, computer assisted surgery. Arch Otorhinolaryng [Suppl] 2:45
198. Schreiner S, Galloway RL Jr, Lewis JT, Bass WA, Muratore DM (1998) An ultrasound approach to localization of fiducial markers for interactive image-guided neurosurgery. Part II: Implementation and automation. IEEE Trans Biomed Eng 45:631–641
199. Schröder HW, Gaab MR (1999) Endoscopic aqueductoplasty: technique and results. Neurosurgery 45:508–515
200. Schul C, Wassermann H, Skopp GB, Marinov M, Wolfer J, Schuierer G, Joos U, Willich N (1998) Surgical management of intraosseous skull base tumors with aid of operating arm system. Comput Aided Surg 3:312–319
201. Smith KP, Frank KJ, Bucholz RD (1994) The neurostation—a highly accurate, minimally invasive solution to frameless stereotactic neurosurgery. Comput Med Imaging Graph 18:247–256
202. Schulder M, Maldjian JA, Liu WC, Mun IK, Carmel PW (1997) Functional MRI-guided surgery of intracranial tumors. Stereotact Funct Neurosurg 68:98–105
203. Schulder M, Fontana P, Lavenhar MA, Carmel PW (1999) The relationship of imaging techniques to the accuracy of frameless stereotaxy. Stereotact Funct Neurosurg 72:136–141
204. Selesnick SH, Kacker A (1999) Image-guided surgical navigation in otology and neurotology. Am J Otol 20:688–693
205. Sipos EP, Tebo SA, Zinreich SJ, Long DM, Brem H (1996) In vivo accuracy testing and clinical experience with the ISG viewing wand. Neurosurgery 39:194–202
206. Spetzger U, Laborde G, Gilsbach JM (1995) Frameless neuronavigation in modern neurosurgery. Minim Invas Neurosurg 38:163–166
207. Spiegel EA, Wycis HT, Marks M, Lee AJ (1947) Stereotactic apparatus for operations on the human brain. Science 106:349–350
208. Spiegel EA, Wycis HT (1952) Stereoencephalotomy. Methods and stereotactic atlas of human brain. Grune and Stratton, New York
209. Talairach J, Hecaen H, David M, Monnier M, De Ajuriaguerra J (1949) Recherches sur la coagulation therapeutique des structures sous-corticales chez l'homme. Rev Neurol 81:4–24
210. Tanaka T, Olivier A, Hashizume K, Hodozuka A, Nakai H (1999) Image-guided epilepsy surgery. Neurol Med Chir (Tokyo) 39:895–900
211. Taren J, Ross D, Lu Y, Harmon L (1995) 3D laser scanning for image guided stereotactic neurosurgery. Acta Neurochir Suppl (Wien) 64:45–48
212. Tebo SA, Leopold DA, Long DM (1996) An optical digitizer for frameless stereotactic surgery. IEEE Comput Graph Applicat 16:55–64
213. Thomas DGT, Doward NL, Kingsley D, Kitchen ND, Palmer JD, Alberti O, Velani B, Hawkes D, Zhao J, Dijkstra A, Gieles P, Buurman J, Gerritsen FA (1997) Clinical experience with the easy guide neuronavigation system. In: Lemke HU, Vannier MW, Inamura K (eds) CAR 97. Elsevier, Amsterdam, pp 757–760
214. Tronnier VM, Wirtz CR, Knauth M, Lenz G, Pastyr O, Bonsanto MM, Albert FK, Kuth R, Staubert A, Schlegel W, Sartor K, Kunze S (1997) Intraoperative diagnostic and interventional magnetic resonance imaging in neurosurgery. Neurosurgery 40:891–902
215. Uematsu S, Lesser R, Fisher RS, Gordon B, Hara K, Kraus GL, Vining EP, Webber RW (1992) Motor and sensory cortex in humans: topography studied with chronic subdural stimulation. Neurosurgery 31:59–72
216. Ungersboeck K, Aichholzer M, Günthner M, Rössler K, Görzer H, Koos WT (1997) Cavernous malformations: from frame-based to frameless stereotactic localization. Minim Invasive Neurosurg 40:134–138
217. van Herk M, Kooy HM (1994) Automatic three dimensional correlation of CT-CT, CT-MRI, CT-SPECT using chamfer matching. Med Phys 21:1163–1178
218. Vannier MW, Haller JW (1999) Navigation in diagnosis and therapy. Eur J Radiol 31:132–140
219. van Roost D, Schaller C, Meyer B, Schramm J (1997) Can neuronavigation contribute to standardization of selective amygdalohippocampectomy? Stereotact Funct Neurosurg 69:239–242
220. Villalobos H, Germano IM (1999) Clinical evaluation of multimodality registration in frameless stereotaxy. Comput Aided Surg 4:45–49
221. Vrionis FD, Foley KT, Robertson JH, Shea JJ (1997) Use of cranial surface anatomic fiducials for interactive image-guided navigation in the temporal bone: a cadaveric study. Neurosurgery 40:755–763
222. Wadley JP, Dorward NL, Breeuwer M, Gerritsen FA, Kitchen ND, Thomas DGT (1998) Neuronavigation in 210 cases: further development of applications and full integration into contemporary neurosurgical practice. In: Lemke HU, Vannier MW, Inamura K, Farman A (eds) CAR 98. Elsevier, Amsterdam, pp 635–640
223. Wadley J, Kitchen N, Thomas D (1999) Image-guided neurosurgery. Hosp Med 60:34–38
224. Wadley J, Dorward N, Kitchen N, Thomas D (1999) Preoperative and intraoperative guidance in modern neurosurgery: a review of 300 cases. Ann R Coll Surg Engl 81:217–225
225. Wagner W, Tschiltschke W, Niendorf WR, Schroeder HWS, Gaab MR (1997) Infrared-based neuronavigation and cortical motor stimulation in the management of central-region tumours. Stereotact Funct Neurosurg 68:112–116
226. Wagner W, Gaab MR, Schroeder HW, Sehl U, Tschiltschke W (1999) Experiences with cranial neuronavigation in pediatric neurosurgery. Pediatr Neurosurg 31:231–236

227. Warnick R (1997) The cost-effectiveness of image-guided craniotomy for metastatic brain tumors workshop. November 8–10, Mainz (personal communication)
228. Wells TH, Cosman ER, Ball RE (1987) The Brown-Roberts-Wells (BRW) arc: its concept as a spatial navigation system. Appl Neurophysiol 50:127–132
229. Wang MY, Maurer CR Jr, Fitzpatrick JM, Maciunas RJ (1996) An automatic technique for finding and localizing externally attached markers in CT and MR volume images of the head. IEEE Trans Biomed Eng 43:627–637
230. Watanabe E, Watanabe T, Manaka S, Mayanagi Y, Takakura K (1987) Three-dimensional digitizer (neuronavigator): new equipment for computed tomography-guided stereotactic surgery. Surg Neurol 27:543–547
231. Watanabe E, Mayanagi Y, Kosugi Y, Manaka S, Takakura K (1991) Open surgery assisted by the neuronavigator, a stereotactic, articulated, sensitive arm. Neurosurgery 28:792–800
232. Westermann B, Hauser R (1997) Precise tracking of an operating microscope for intranasal image guided surgery: improved accuracy with a laser-supported method. In: Lemke HU, Vannier MW, Inamura K (eds) CAR 97. Elsevier, Amsterdam, pp 878–883
233. Westermann B, Hauser R (1996) Non-invasive 3D patient registration for image-guided skull base surgery. Comput Graph 20:793–799
234. Westermann B, Trippel M, Reinhardt H (1995) Optically navigable operating microscope for image-guided surgery. Minim Invas Neurosurg 38:112–116
235. Wichmann MW (1967) The use of optical feedback in computer control of an arm. Standford Artificial Intelligence Laboratory, Standford University, AIM 56
236. Wirtz CR, Tronnier VM, Bonsanto MM, Knauth M, Staubert A, Kunze S (1997) Image-guided neurosurgery with intraoperative MRI: update of frameless stereotaxy and radicality control. Stereotact Funct Neurosurg 68:39–43
237. Wirtz CR, Tronnier VM, Bonsanto MM, Hassfeld S, Knauth M, Kunze S (1998) Neuronavigation. Methods and prospects. Nervenarzt 69:1029–1036
238. Wirtz CR, Knauth M, Hassfeld S, Tronnier VM, Albert FK, Bonsanto MM, Kunze S (1998) Neuronavigation. First experiences with three different commercially available systems. Zentralbl Neurochir 59:14–22
239. Wolf M, Heissler E, Wust P, Beier J, Stahl H, Felix R, Bier J (1997) Test of navigation systems for image-guided implantation of catheters. In: Lemke HU, Vannier MW, Inamura K (eds) CAR 97. Elsevier, Amsterdam, pp 909–913
240. Wurm G, Wies W, Schnizer M, Trenkler J, Holl K (2000) Advanced surgical approach for selective amygdalohippocampectomy through neuronavigation. Neurosurgery 46:1377–1382
241. Yasargil MG (1984) Microneurosurgery, vol 1. Thieme, Stuttgart
242. Yasargil MG (1984) Microneurosurgery, vol 2. Thieme, Stuttgart
243. Yasargil MG (1987) Microneurosurgery, vol 3A. Thieme, Stuttgart
244. Yasargil MG (1988) Microneurosurgery, vol 3B. Thieme, Stuttgart
245. Yasargil MG (1994) Microneurosurgery, vol 4A. Thieme, Stuttgart
246. Yasargil MG (1996) Microneurosurgery, vol 4B. Thieme, Stuttgart
247. Young RF (1987) Application of robotics to stereotactic neurosurgery. Neurol Res 9:123–128
248. Zamorano L, Nolte LP, Kadi AM (1993) Interactive intraoperative localization using infrared-based system. Neurol Res 15:290–298
249. Zamorano L, Jiang C, Chavantes C, Diaz FG (1999) Stereotactic and interactive image-guided neuroendoscopy. In: Alexander E III, Maciunas RJ (eds) Advanced neurosurgical navigation. Thieme, New York, pp 311–320
250. Zeilenhofer HF, Krol Z, Sader R, Hoffmann KH, Hogg M, Schwaiger M, Gerhardt P, Horch HH (1997) Multimodal images in diagnostics of head and neck area using efficient registration and visualization methods. In: Lemke HU, Vannier MW, Inamura K (eds) CAR 97. Elsevier, Amsterdam, pp 723–728
251. Zernov DN (1890) L'encephalometrie. Rev Gen Clin Ther 19:302
252. Zinreich SJ, Tebo SA, Long DM, Brem H, Mattox DE, Loury ME, Van der Kolk CA, Koch WM, Kennedy DW, Bryan RN (1993) Frameless stereotactic integration of CT imaging data: accuracy and initial applications. Radiology 188:735–742